Electronic Supplementary Material (ESI) for RSC Advances.

Supporting Information

Arene Platform Based Hexa-amide Receptors for Anion Recognition: Single Crystal X-ray Structural and Thermodynamic Studies

Sourav Chakraborty[a], M. Arunachalam[a], Ranjan Dutta[a], and Pradyut Ghosh[a]*

[a] Department of Inorganic Chemistry Indian Association for the Cultivation of Science, 2A & 2B Raja S. C. Mullick Road, Kolkata 700032, India. Fax: (+91) 33-2473-2805, E-mail: icpg@iacs.res.in.

Table of contents

Materials: All reagents, tetrabutylammonium salts, and solvents for syntheses were purchased from commercial sources and used as received. Freshly dried tetrahydrofuran was used for each reaction. The solvents used for crystallisation were all of HPLC grade.

Instrumentation: ^{1}H NMR spectra were recorded with a 300 MHz Bruker DPX-300. ^{13}C NMR spectra were obtained at 75.47 MHz. HRMS experiments were carried out on a Waters QtoF Model YA 263 mass spectrometer in positive ESI mode. Elemental analyses for the synthesized ligand and complexes were carried out with a Perkin-Elmer 2500 series II elemental analyzer. ITC experiments were performed in VP-ITC instrument.

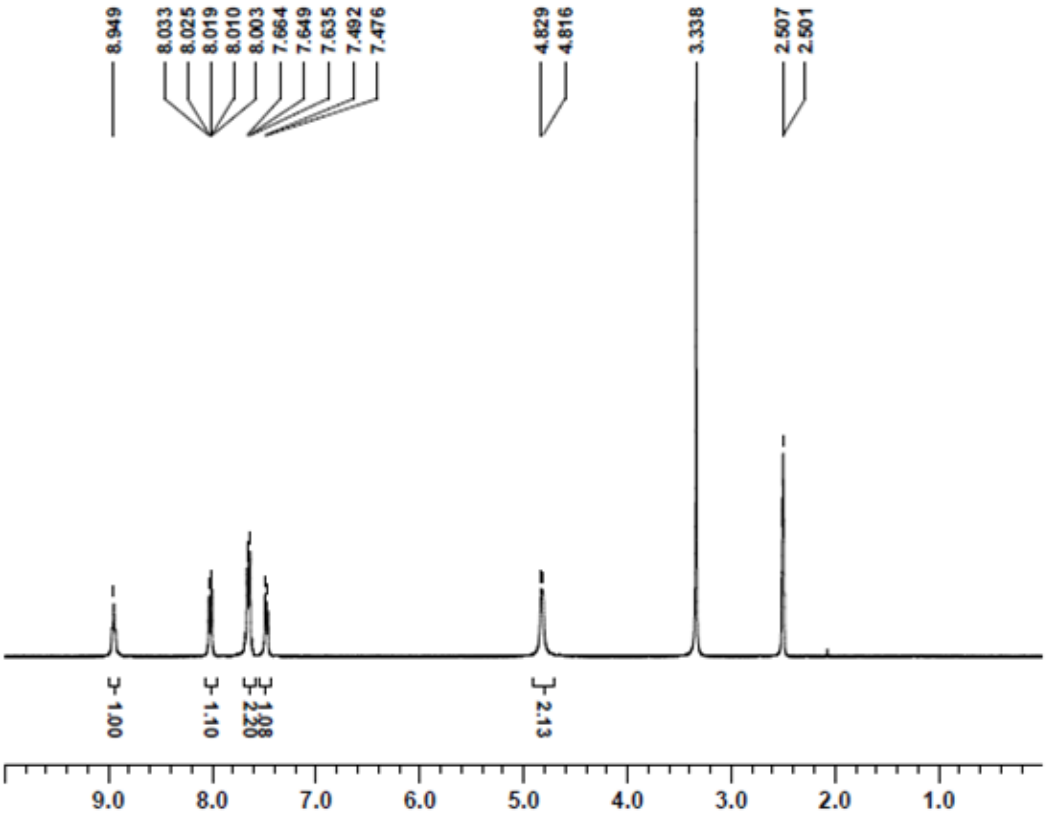

Fig. 1S: ^{1}H NMR (300 MHz) spectrum of receptor **L1** in DMSO-d_6 at 25°C.

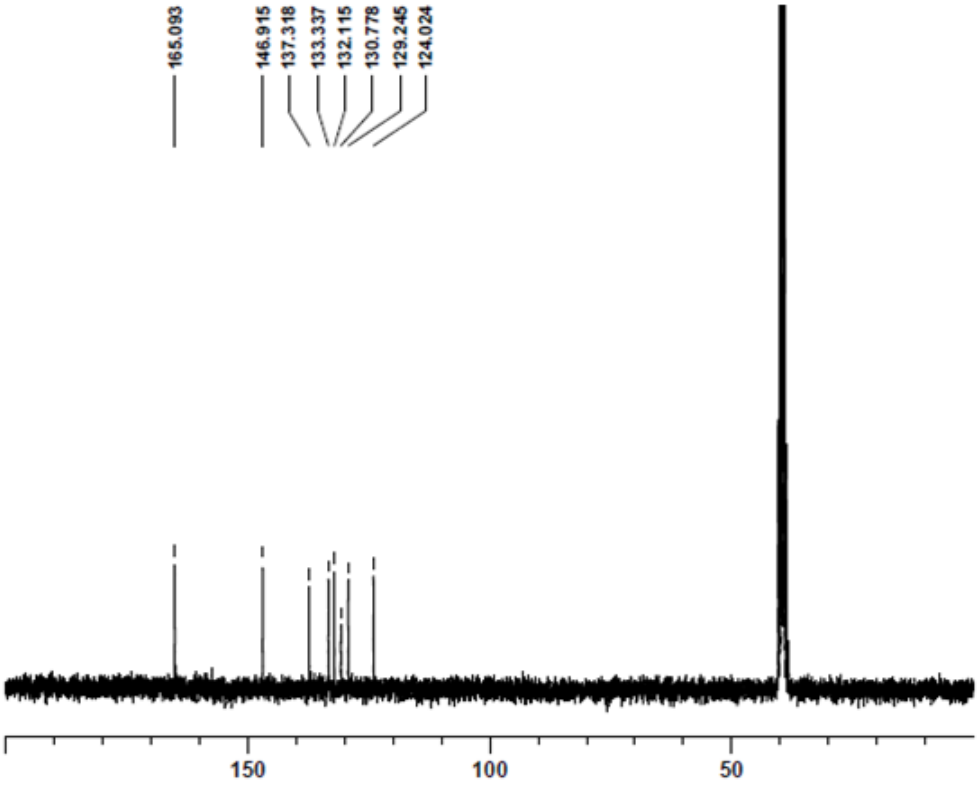

Fig. 2S: ^{13}C NMR (75 MHz) spectrum of receptor **L1** in DMSO-d_6 at 25°C.

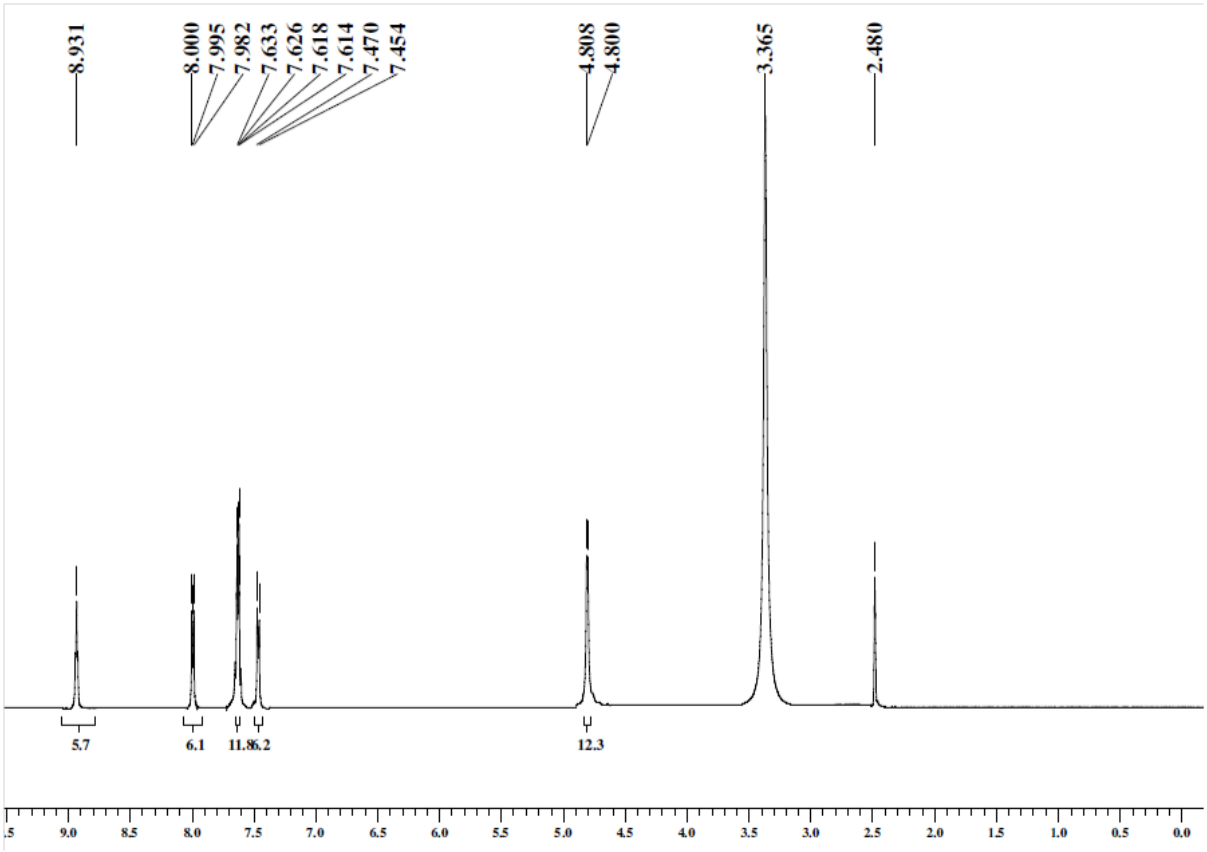

Fig. 3S: ^{1}H NMR (300 MHz) spectrum of receptor **L2** in DMSO-d_6 at 25°C.

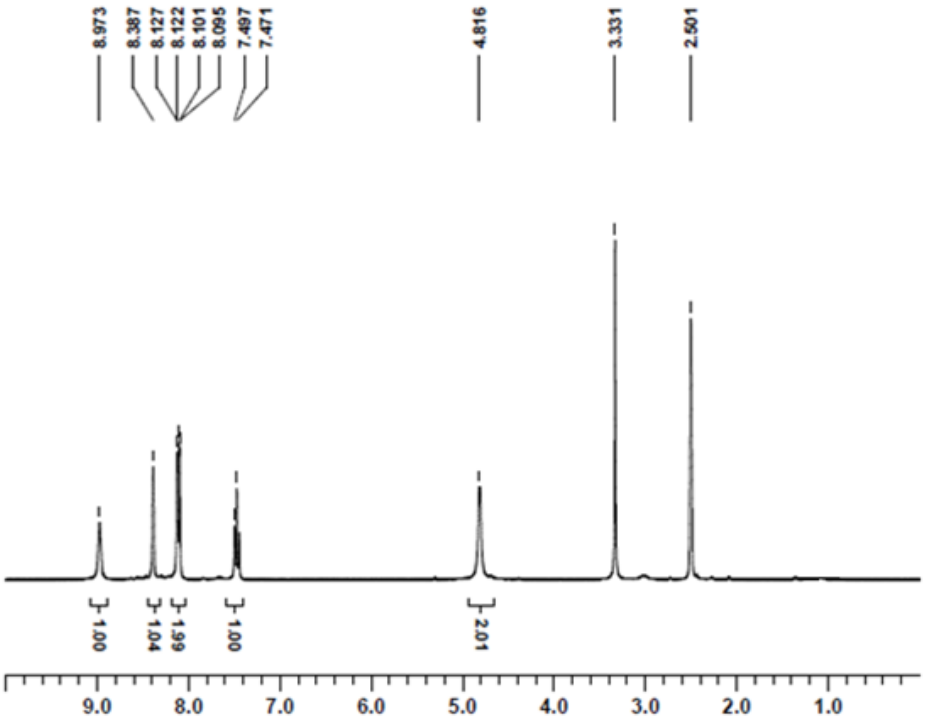

Fig. 4S: ^{1}H NMR (300 MHz) spectrum of receptor **L3** in DMSO-d_6 at 25°C.

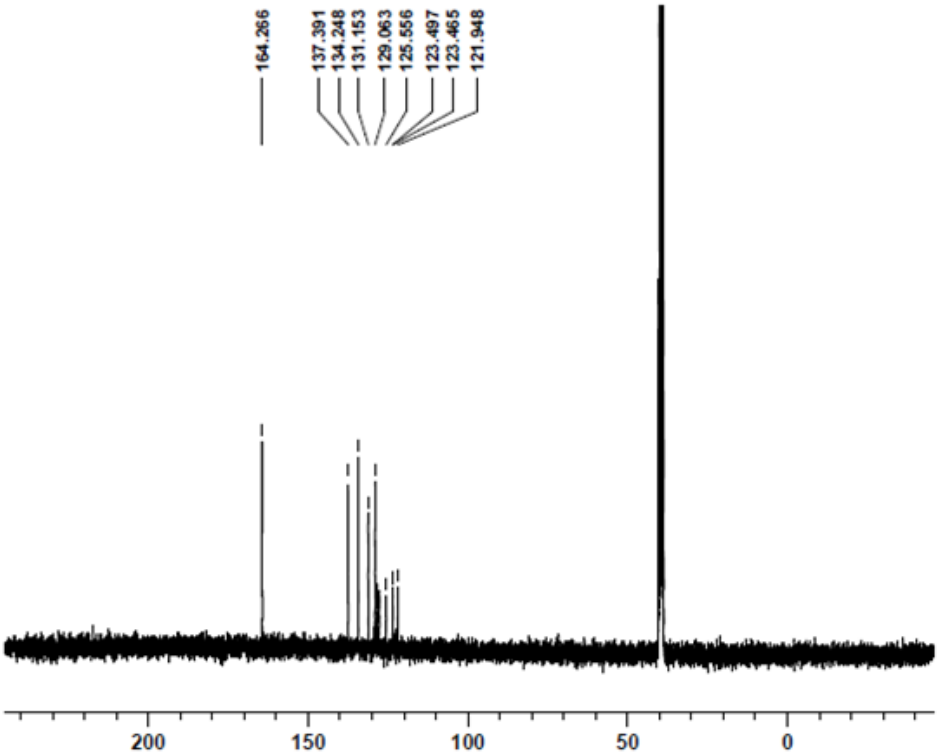

Fig. 5S: ^{13}C NMR (75 MHz) spectrum of receptor **L3** in DMSO-d_6 at 25°C.

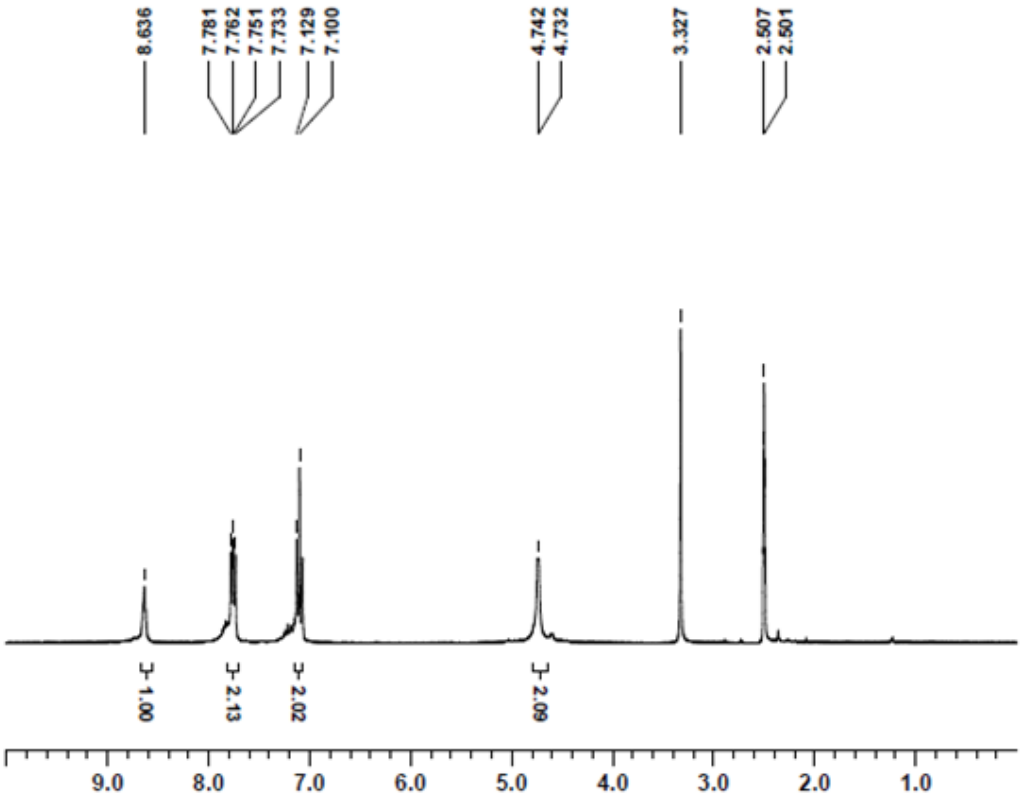

Fig. 6S: ^{1}H NMR (300 MHz) spectrum of receptor **L4** in DMSO-d_6 at 25°C.

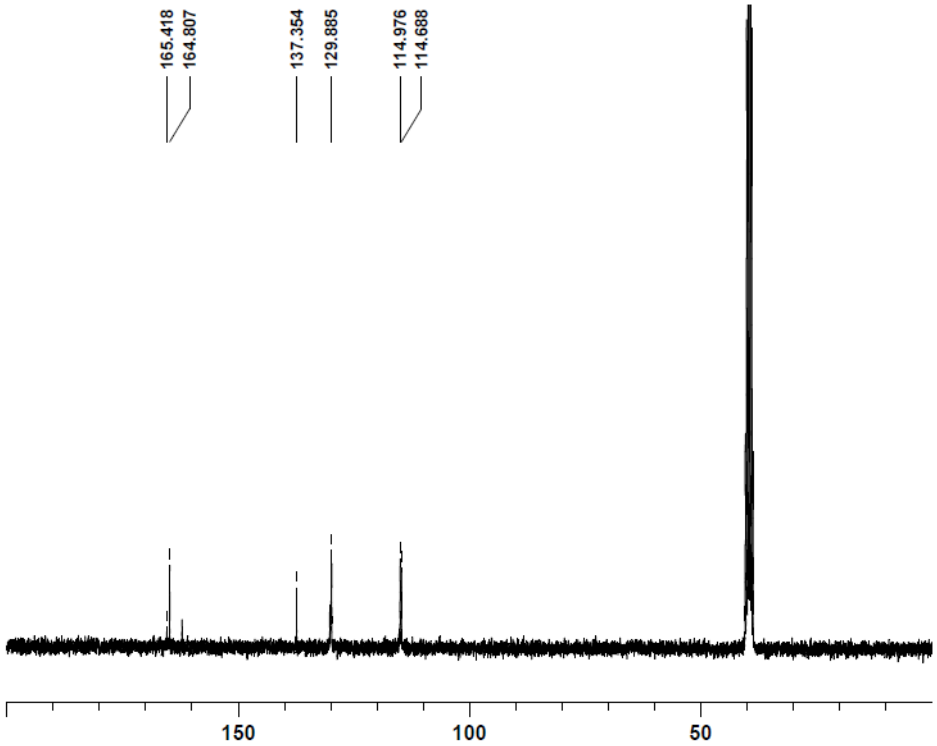

Fig. 7S: ^{13}C NMR (75 MHz) spectrum of receptor **L4** in DMSO-d_6 at 25°C.

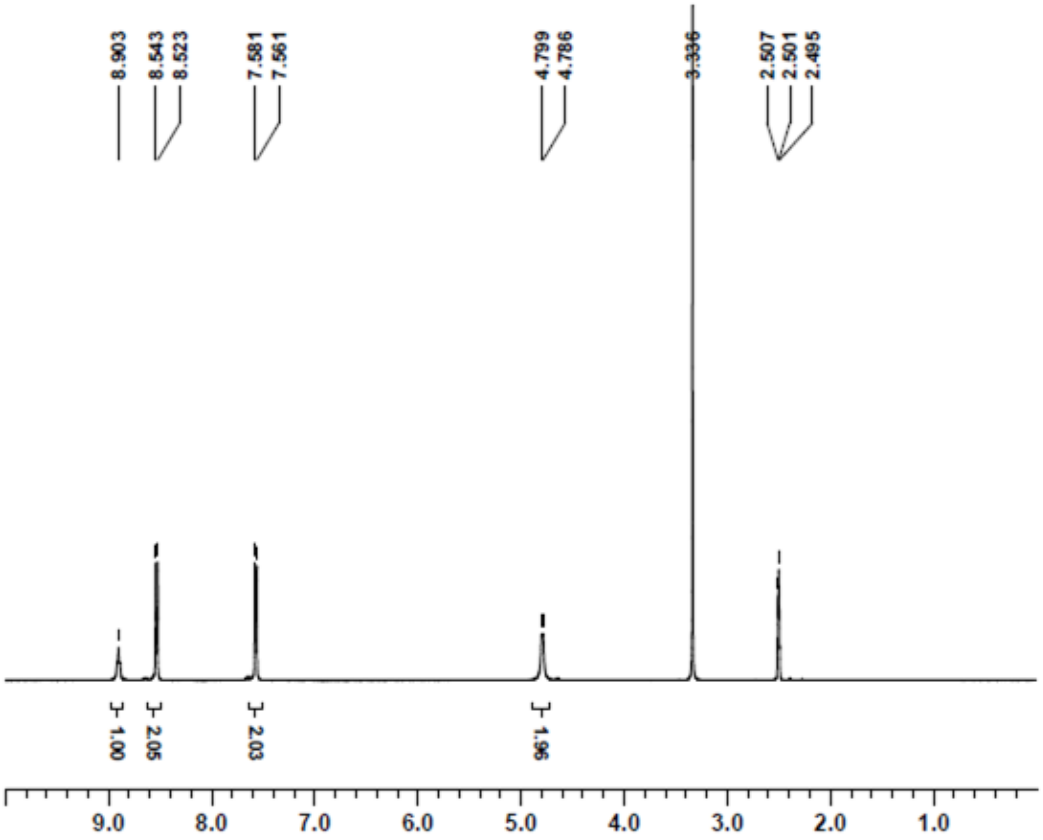

Fig. 8S: ^{1}H NMR (300 MHz) spectrum of receptor **L5** in DMSO-d_6 at 25°C.

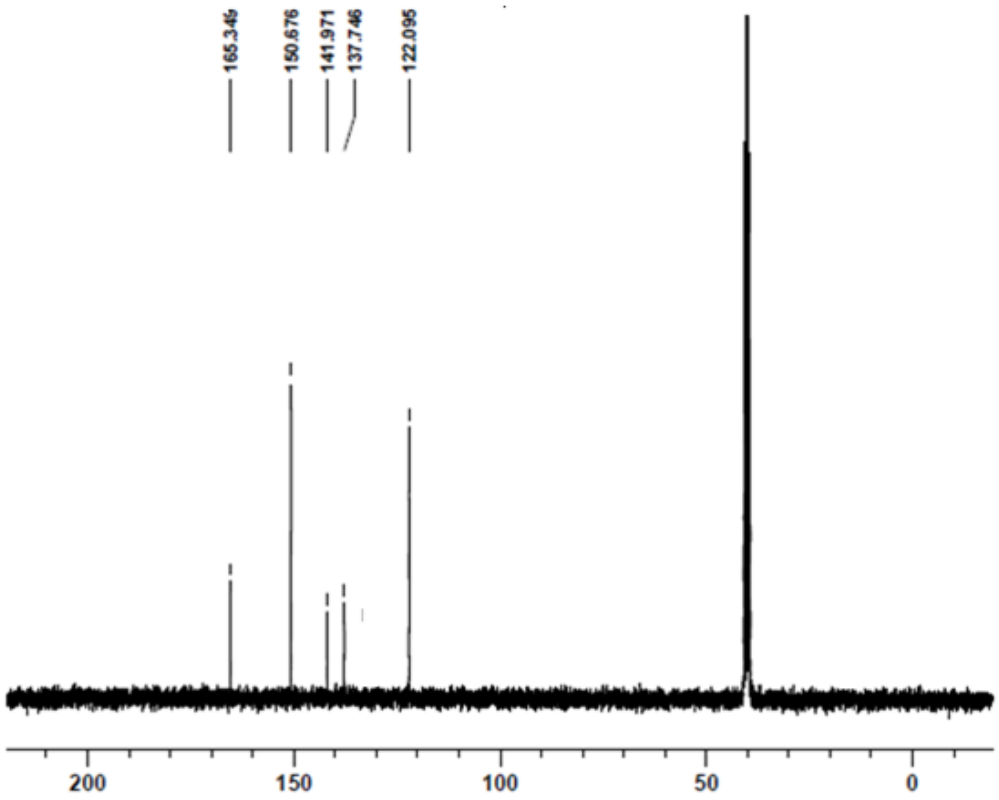

Fig. 9S: ^{13}C NMR (75 MHz) spectrum of receptor **L5** in DMSO-d_6 at 25°C.

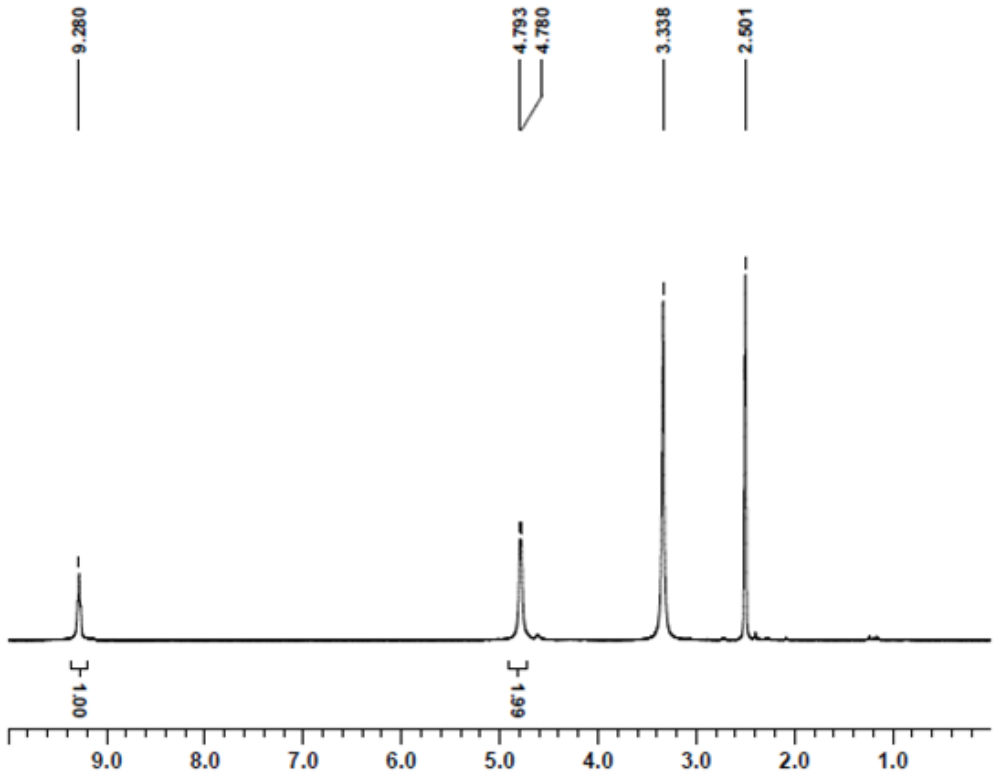

Fig. 10S: ^{1}H NMR (300 MHz) spectrum of receptor **L6** in DMSO-d_6 at 25°C.

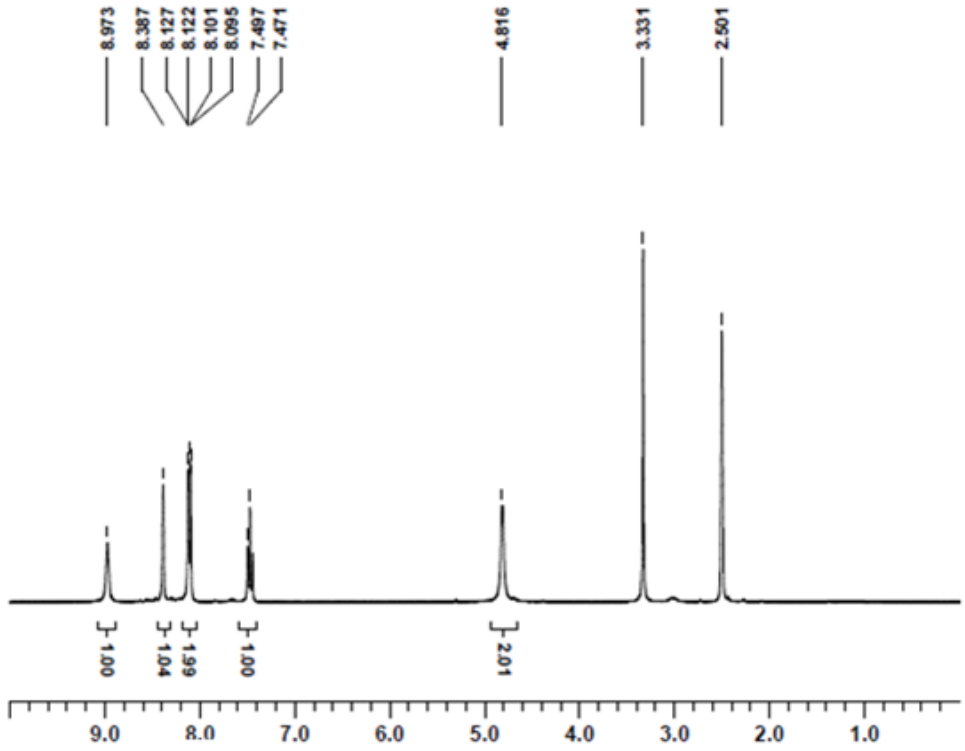

Fig. 11S: ^{1}H NMR (300 MHz) spectrum of receptor **L7** in DMSO-d_6 at 25°C.

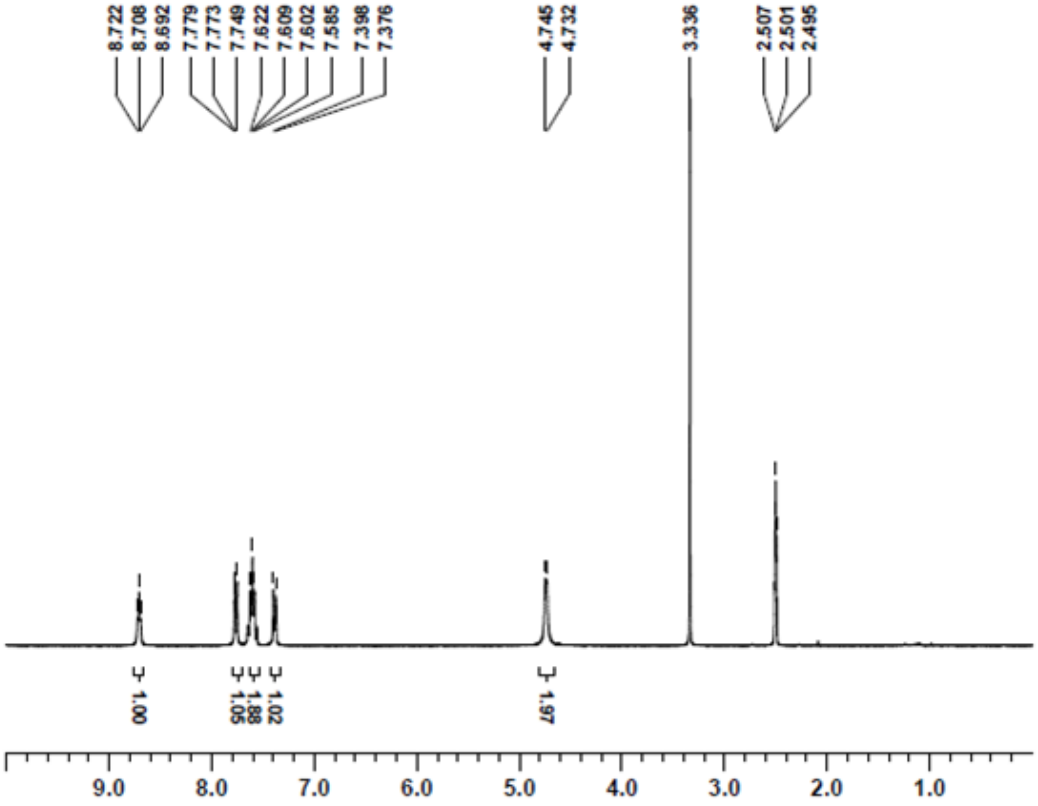

Fig. 12S: ^{1}H NMR (300 MHz) spectrum of receptor **L8** in DMSO-d_6 at 25°C.

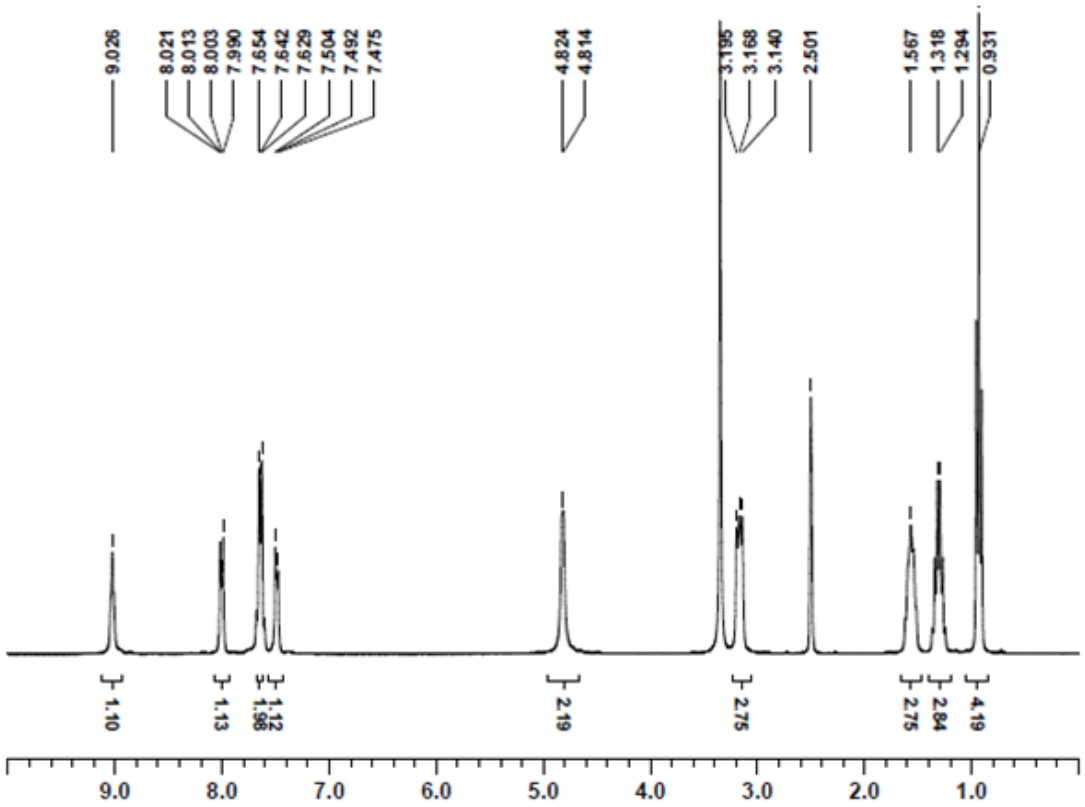

Fig. 13S: ^{1}H NMR (300 MHz) spectrum of receptor **Complex 1** in DMSO-d_6 at 25°C.

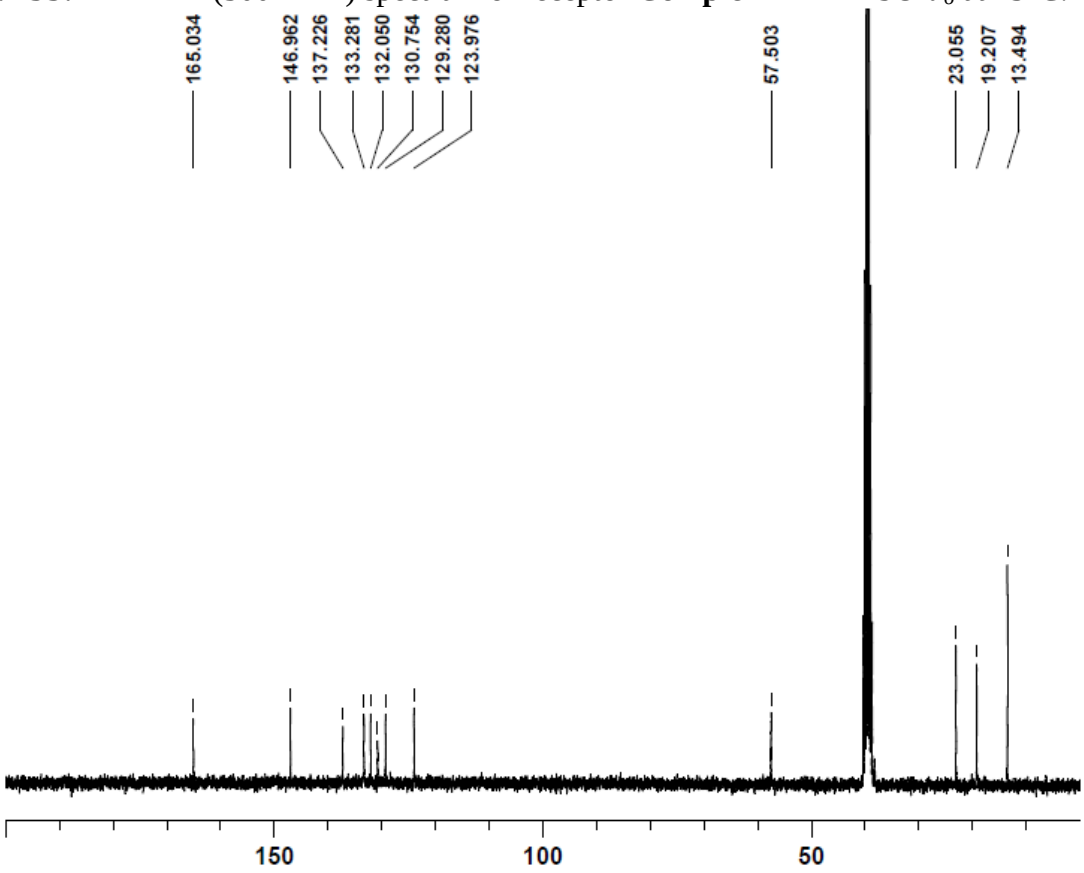

Fig. 14S: ^{13}C NMR (75 MHz) spectrum of receptor **Complex 1** in DMSO-d_6 at 25°C.

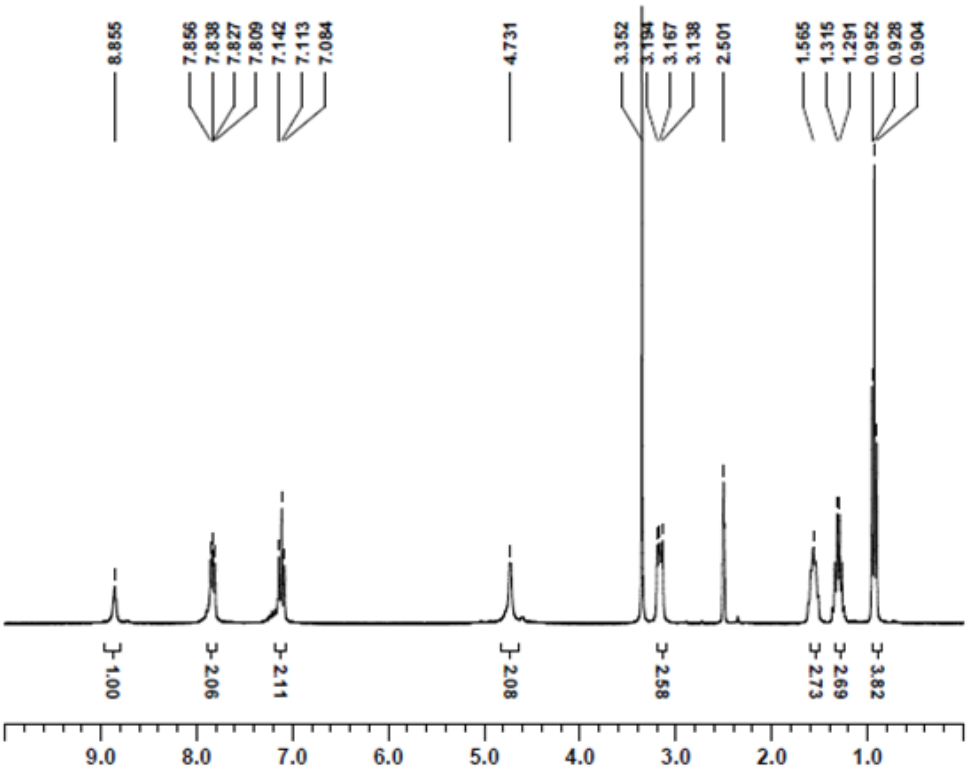

Fig. 15S: ^{1}H NMR (300 MHz) spectrum of receptor **Complex 2** in DMSO-d_6 at 25°C.

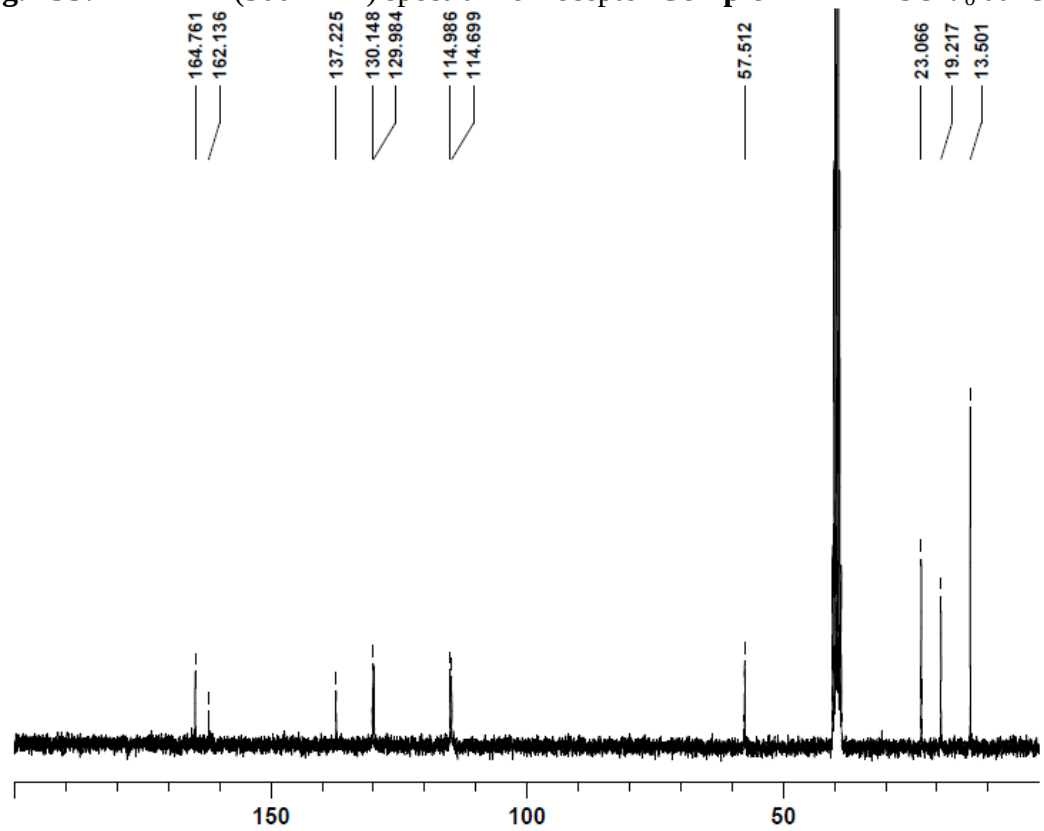

Fig. 16S: ^{13}C NMR (75 MHz) spectrum of receptor **Complex 2** in DMSO-d_6 at 25°C.

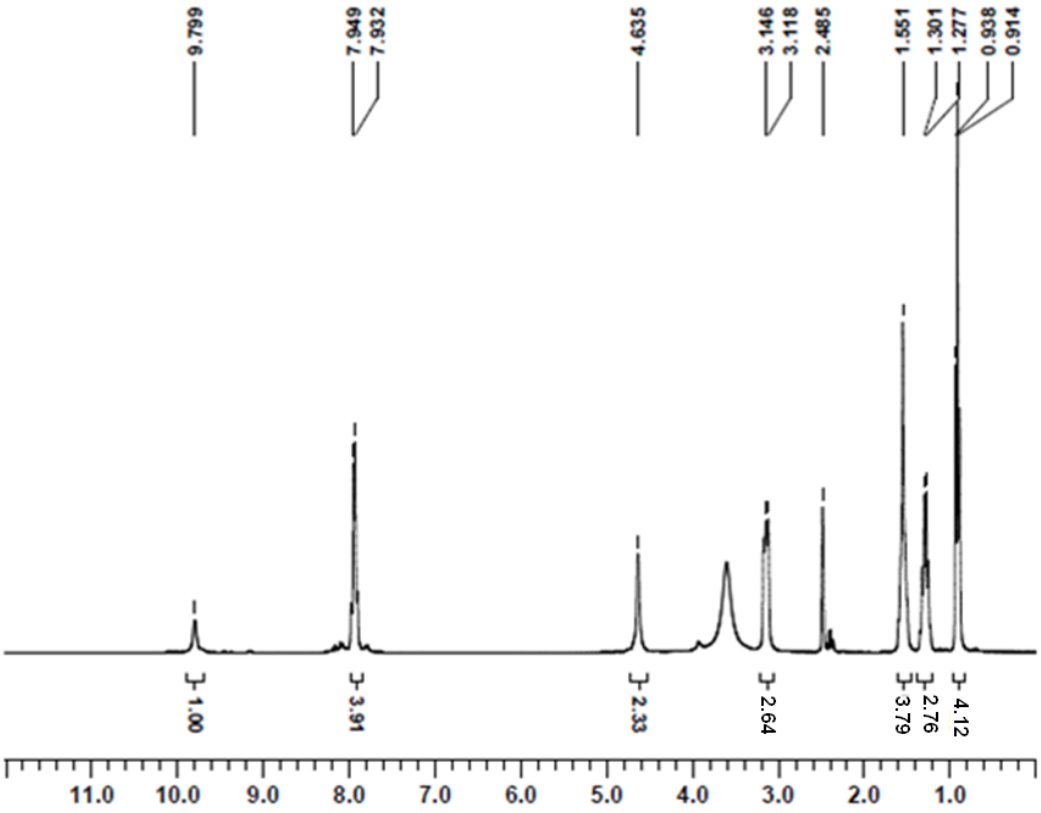

Fig. 17S: ^{1}H NMR (300 MHz) spectrum of receptor **Complex 3** in DMSO-d_6 at 25°C.

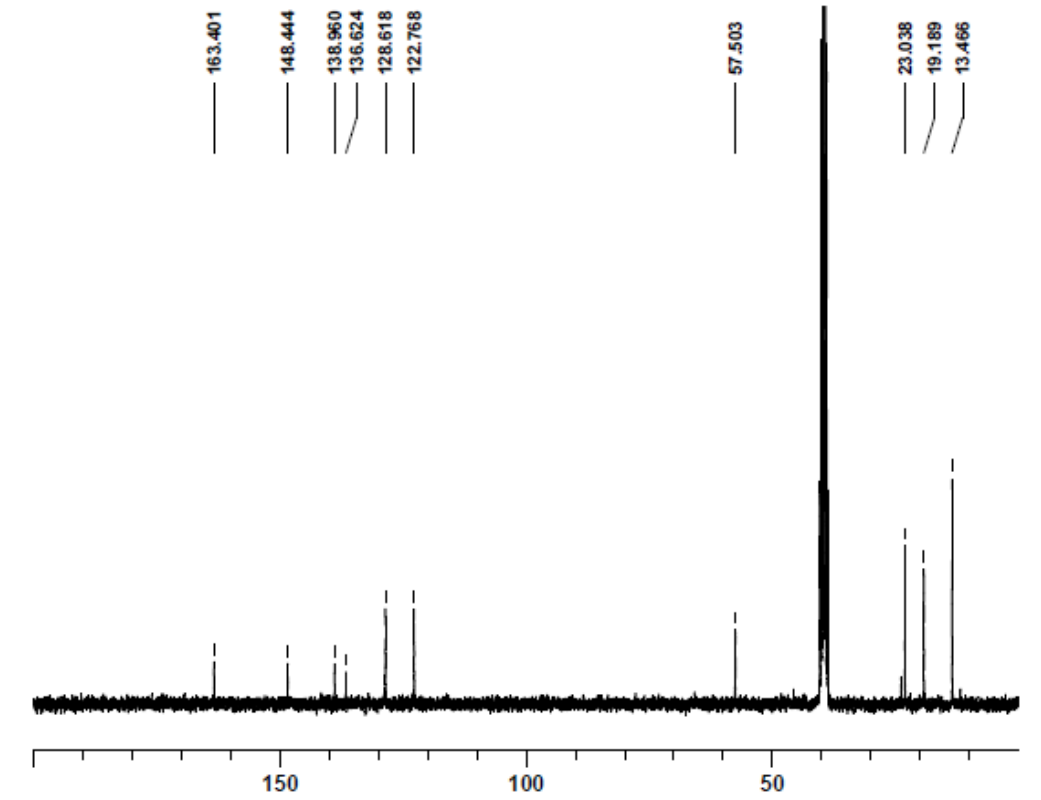

Fig. 18S: ^{13}C NMR (75 MHz) spectrum of receptor **Complex 3** in DMSO-d_6 at 25°C.

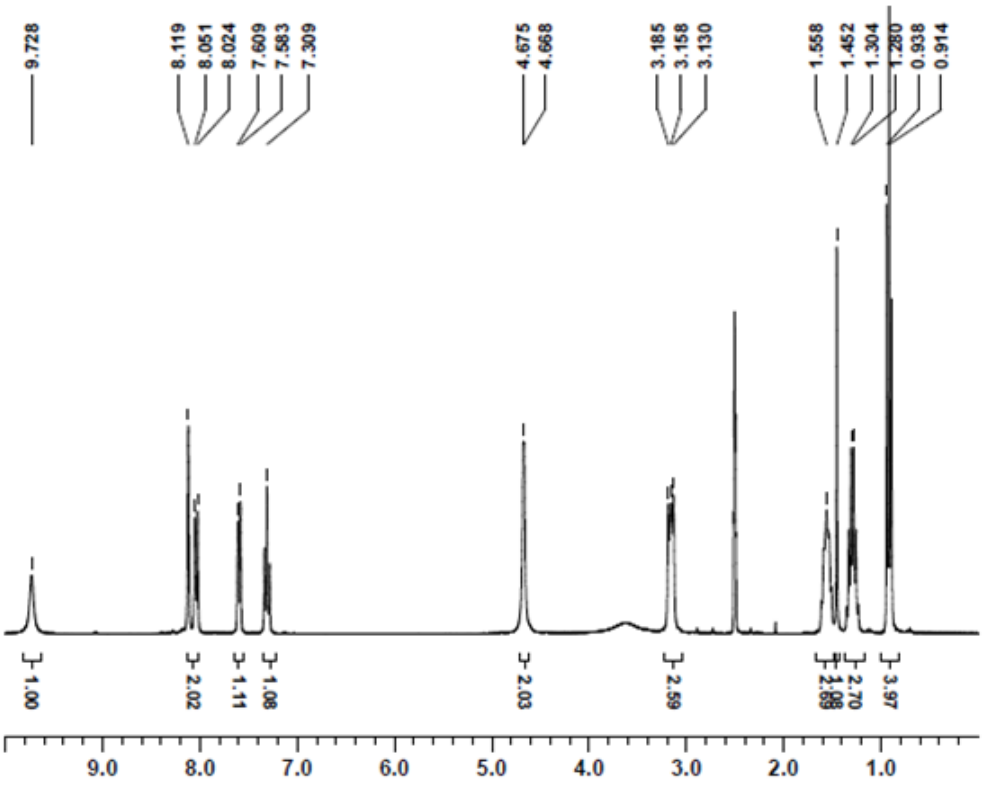

Fig. 19S: ^{1}H NMR (300 MHz) spectrum of receptor **Complex 4** in DMSO-d_6 at 25°C.

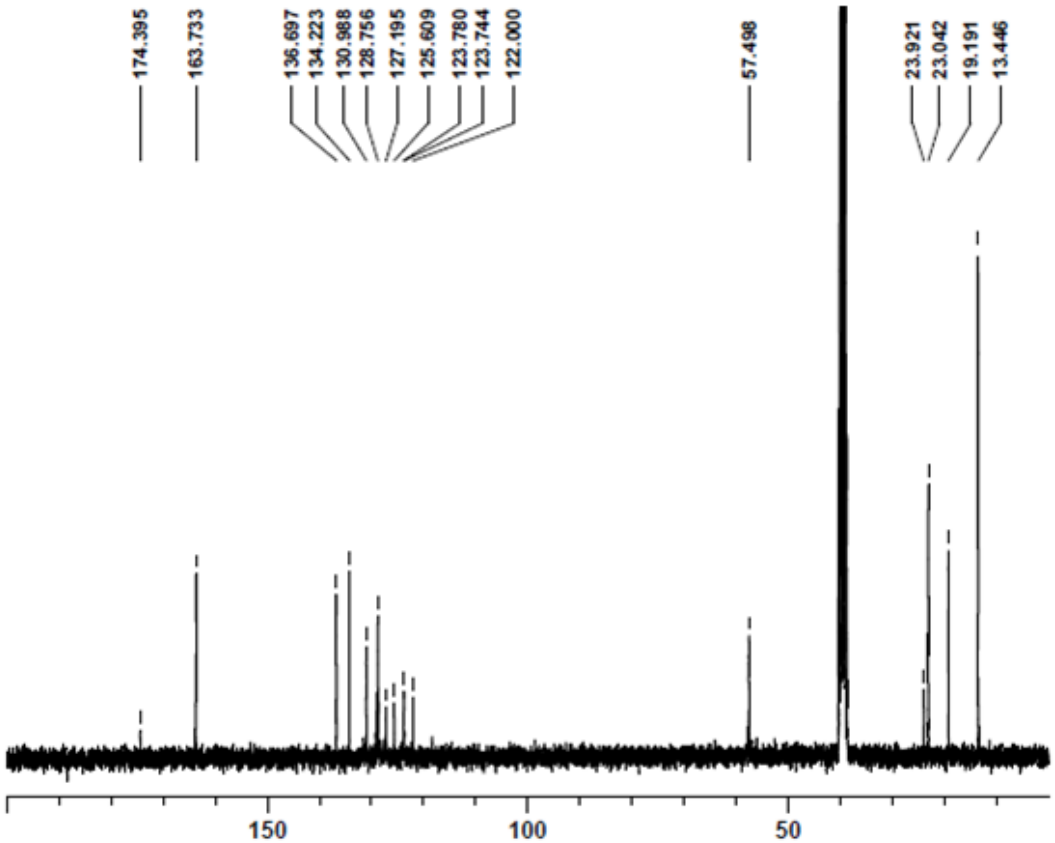

Fig. 20S: ^{13}C NMR (75 MHz) spectrum of receptor **Complex 4** in DMSO-d_6 at 25°C.

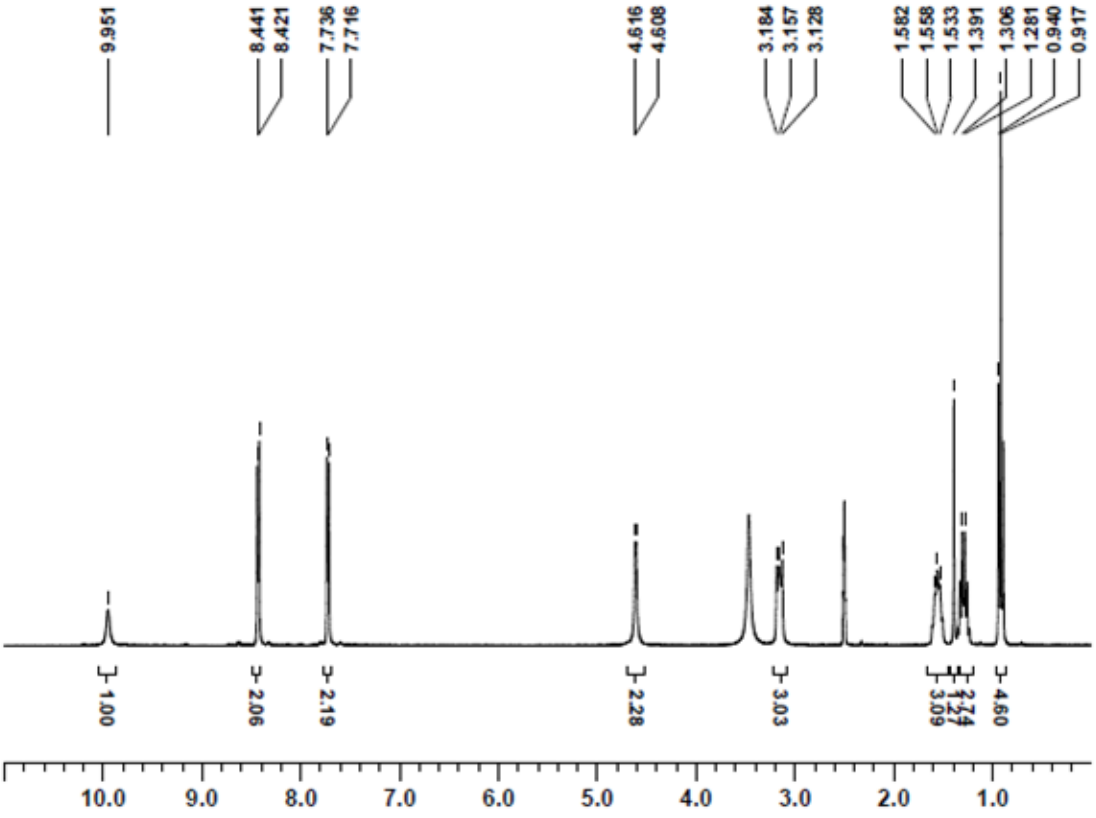

Fig. 21S: ^{1}H NMR (300 MHz) spectrum of receptor **Complex 5** in DMSO-d_6 at 25°C.

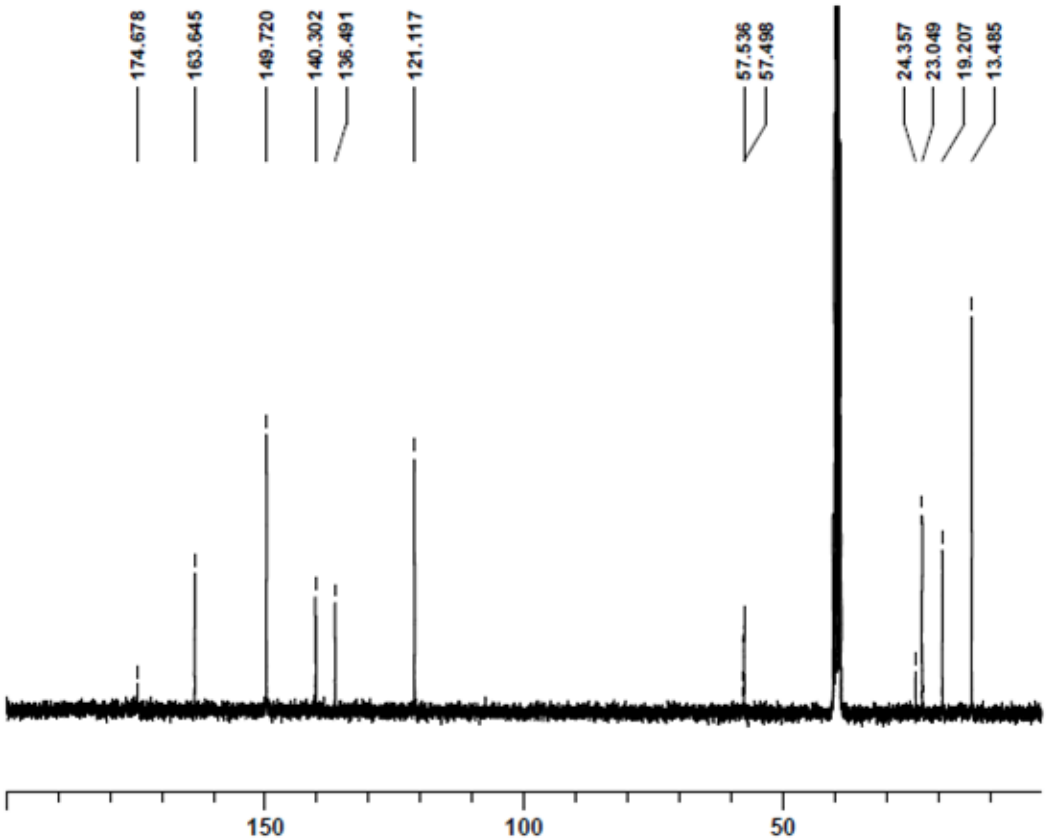

Fig. 22S: ^{13}C NMR (75 MHz) spectrum of receptor **Complex 5** in DMSO-d_6 at 25°C.

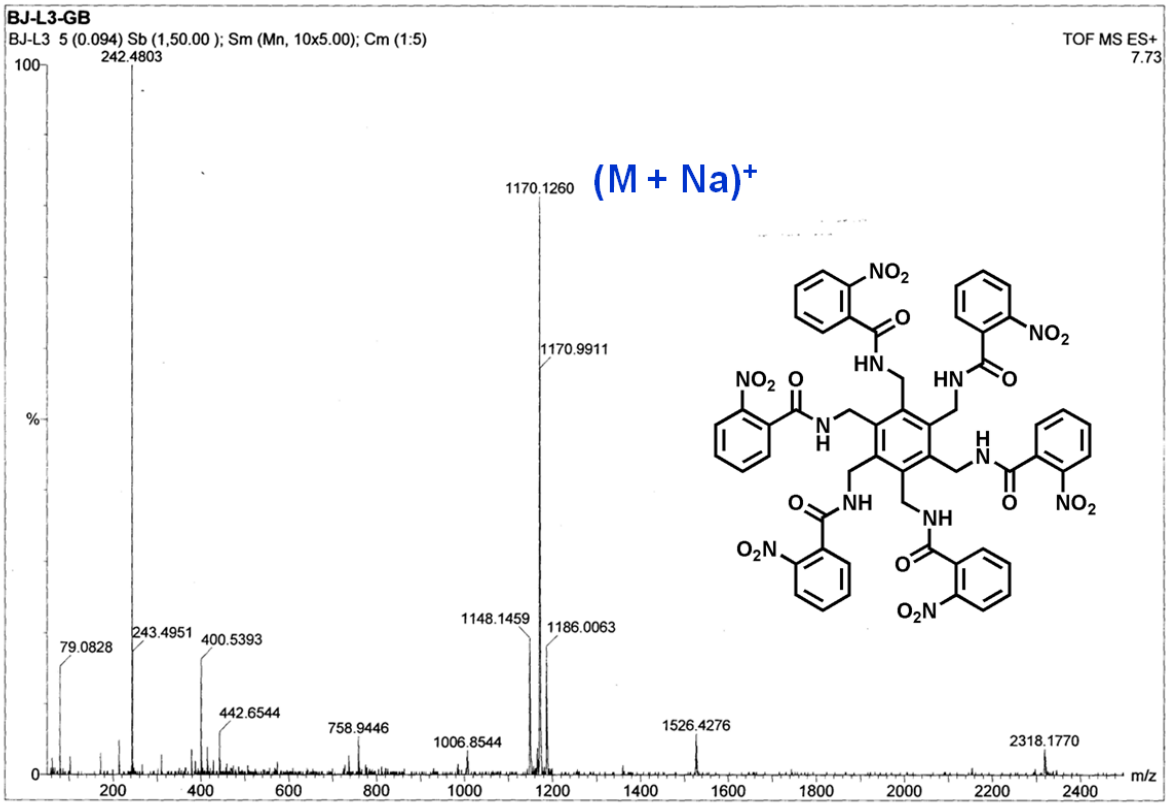

Fig. 23S: HRMS spectrum of **L1**.

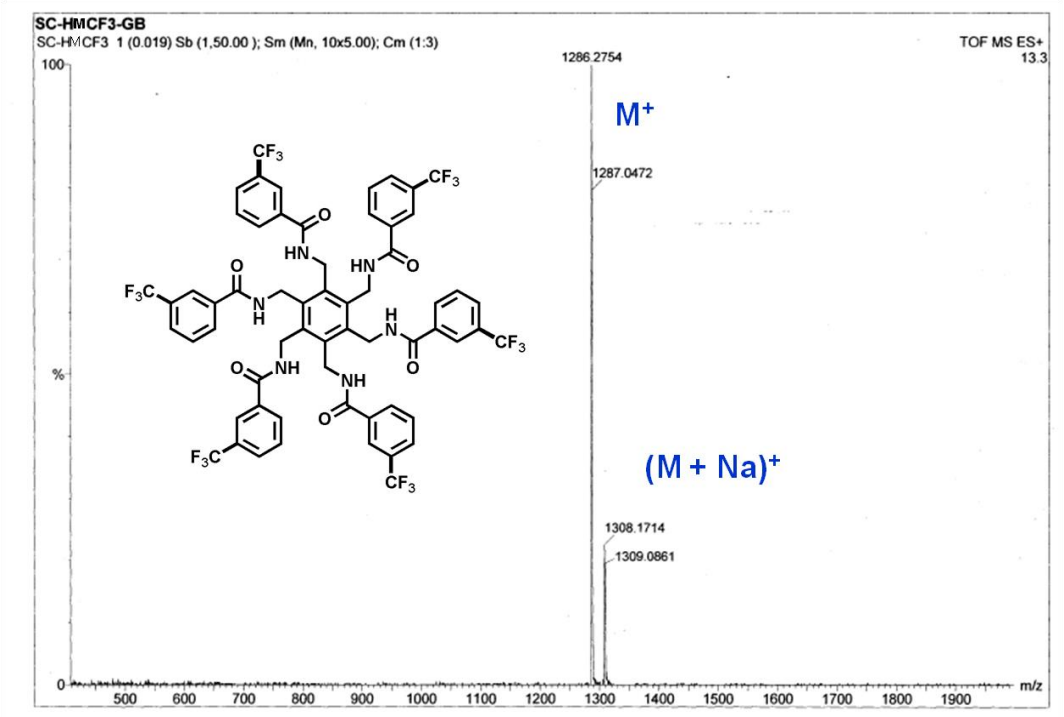

Fig. 24S: HRMS spectrum of **L3**.

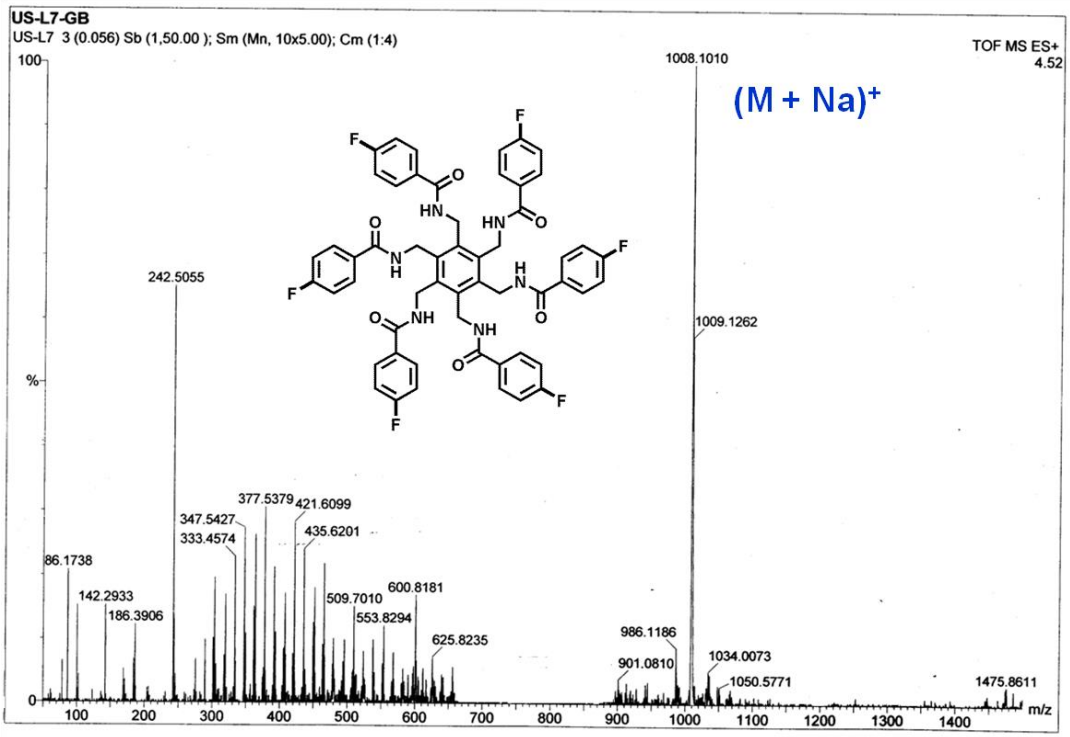

Fig. 25S: HRMS spectrum of **L4**.

Compound reference	**Complex 1**	**Complex 2**	**Complex 3**	**Complex 4**	**complex 5**
Chemical formula	$C_{86}H_{118}Cl_2N_{14}O_{20}$	$C_{118}H_{186}Cl_2F_6N_{10}O_{16}$	$C_{90}H_{120}N_{14}O_{26}$	$C_{96}H_{120}F_{18}N_8O_{14}$	$C_{90}H_{132}N_{14}O_{12}$
Formula Mass	1738.84	2185.67	1814.00	1952.00	1602.10
Crystal system	Monoclinic	Monoclinic	Monoclinic	Triclinic	Triclinic
a/Å	11.195(2)	17.066(10)	38.647(4)	11.425(4)	11.7363(15)
b/Å	15.809(3)	18.946(10)	10.5794(11)	14.397(5)	13.918(4)
c/Å	25.390(4)	20.674(11)	23.724(3)	16.570(6)	15.892(2)
α/°	90.00	90.00	90.00	80.640(10)	109.483(4)
β/°	94.337(5)	105.450(15)	97.545(3)	71.645(10)	110.352(3)
γ/°	90.00	90.00	90.00	89.007(10)	92.310(4)
Unit cell volume/Å^3	4480.7(14)	6443(6)	9615.9(18)	2550.8(17)	2258.3(7)
Temperature/K	120(2)	150(2)	120(2)	150(2)	120(2)
Space group	*P2(1)/c*	*P2(1)/n*	*C2/c*	$P\bar{1}$	$P\bar{1}$
No. of formula units per unit cell, *Z*	2	2	4	1	1
No. of reflections measured	20946	26397	19921	11098	15518
No. of independent reflections	2639	5697	4282	4503	5271
R_{int}	0.0782	0.1341	0.0903	0.0815	0.0525
Final R_1 values ($I > 2\sigma(I)$)	0.0570	0.1084	0.0524	0.0866	0.0491
Final $wR(F^2)$ values ($I > 2\sigma(I)$)	0.1485	0.2837	0.1449	0.2294	0.1223
Final R_1 values (all data)	0.0764	0.1723	0.0926	0.1677	0.0742
Final $wR(F^2)$ values (all data)	0.1660	0.3362	0.1712	0.3092	0.1375
Goodness of fit on F^2	1.070	0.996	1.011	0.856	1.019
CCDC numbers	996873	944134	944137	996872	944133

Table 1S: Crystallographic parameters of the complexes (**1**-**5**).

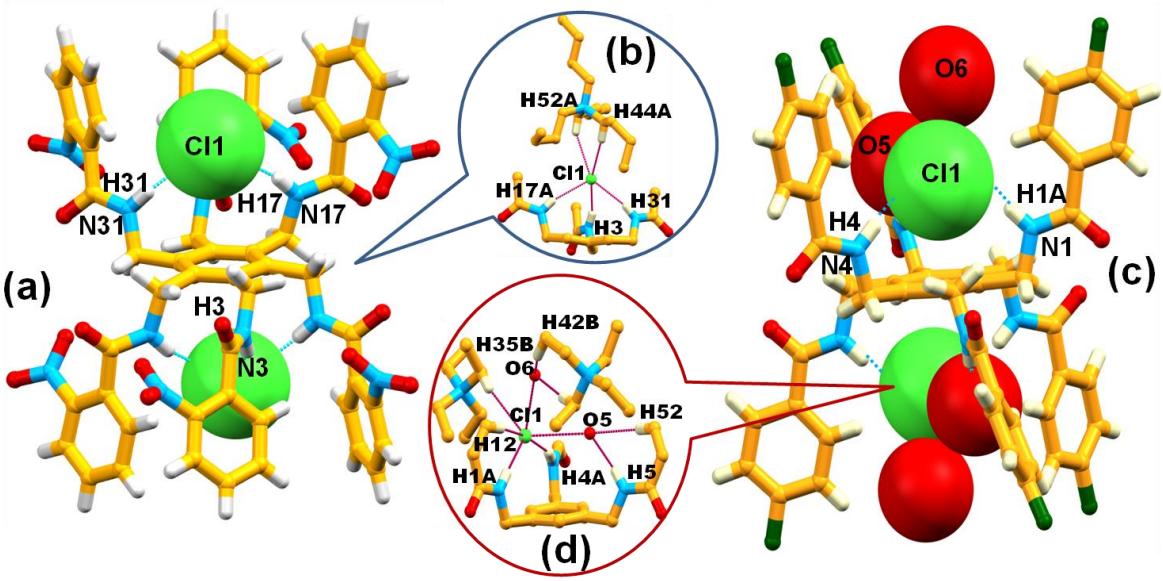

Fig. 26S: (a) *aaabbb* conformation of complex **1** with **L1**; (b) Inset picture showing coordination environment of the chloride in complex **1**; (c) *ababab* conformation of complex **2** which shows recognition of chloride water cluster by **L4**; (d) Inset picture showing coordination environment of the chloride in complex **2**.

.

H-bonding tables of the complexes (**1-5**)

Table 2S: Complex 1			
D-H···A	**H···A (Å)**	**D···A (Å)**	**∠D-H···A (°)**
N3-H3···Cl1[1]	2.31	3.1246	157
N17-H17···Cl1[1]	2.57	3.4056	165
N31-H31···Cl1[2]	2.54	3.3638	161
C23-H23···O33[3]	2.44	3.3472	166
C37-H37···O13[2]	2.52	3.4091	161
C44-H44A···Cl1[4]	2.72	3.6431	160
C48-H48B···O42[5]	2.39	3.2291	144
C52-H52A···Cl1[4]	2.75	3.6288	151
C54-H54B···O2[4]	2.06	3.0220	169
C56-H56A···O19[4]	2.51	3.3519	145
Symmetry codes: (1) 1+x, y, z; (2) 1-x, 1-y, -z; (3) 2-x, 1/2+y, 1/2-z; (4) x, y, z; (5) 1-x,			

Table 3S: Complex 2			
D-H···A	**H···A (Å)**	**D···A (Å)**	**∠D-H···A (°)**
N1-H1A···Cl1[1]	2.56	3.3709	157
N4-H4A···Cl1[2]	2.49	3.3149	162
N5-H5···O5[2]	2.11	2.9641	171
C12-H12···Cl1[1]	2.81	3.6851	158
C15-H15A···O4[3]	2.55	3.4982	165
C19-H19B···O26A[4]	2.39	3.2520	147
C21-H21A···F1[4]	2.49	3.3442	147
C23-H23A···O1[3]	2.29	3.1852	153
C23-H23B···O4[3]	2.45	3.4192	177
C31-H31B···O6[5]	2.56	3.5252	176

C35-H35B···Cl1[6]	2.75	3.6491	154
C42-H42B···O6[5]	2.43	3.2482	142
C52-H52···O5[2]	2.42	3.2482	149
Symmetry codes: (1) 1/2-x, -1/2+y, 1/2-z; (2) -1/2+x, 1/2-y, 1/2+z; (3) 1/2-x, 1/2+y, 1/2-z; (4) -1/2+x, 1/2-y, -1/2+z; (5) x, y, z ; (6) 3/2-x, -1/2+y, 1/2-z.			

Table 4S: Complex 3			
D-H···A	**H···A (Å)**	**D···A (Å)**	**∠D-H···A (°)**
N8-H8···O1[1]	2.27	2.9015	130
N23-H23···O1[1]	2.02	2.8495	161
N37-H37···O3[2]	2.05	2.8936	166
C13-H13···O33[2]	2.55	3.3248	141
C28-H28···O20[2]	2.54	3.3327	144
C31-H31···O1[1]	2.51	3.3406	149
C50-H50B···O10[3]	2.44	3.3206	151
C55-H55A···O10[3]	2.58	3.4776	154
C58-H58A···O25[4]	2.35	3.2997	166
C59-H59A···O5A[1]	2.51	3.4218	157
C59-H59B···O47[1]	2.49	3.2287	132
C62-H62A···O47[1]	2.44	3.4137	177
C63-H63B···O25[4]	2.54	3.4336	154
Symmetry codes: (1) x, y, z; (2) 1/2-x,1/2-y,2-z; (3) x,-y,-1/2+z; (4) x,1-y,-1/2+z.			

Table 5S: Complex 4			
D-H···A	**H···A (Å)**	**D···A (Å)**	**∠D-H···A (°)**
N--H1···O5[1]	2.11	2.9241	157
N2-H2A···O5[4]	1.96	2.8008	166

N3-H3A···O4[4]	2.00	2.8307	162
C2-H2···O5[1]	2.52	3.4257	166
C16-H16···O5[4]	2.31	3.1898	158
C23-H23···O4[4]	2.58	3.3630	142
C30-H30A···O1[4]	2.46	3.4298	173
C34-H34A···O2[2]	2.49	3.4416	168
C34-H34B···O7[3]	2.46	3.3972	162
C38-H38B···O3[4]	2.55	3.4480	153
Symmetry codes: (1) 1-x, -y, 1-z; (2) -1+x, y, z; (3) 1-x, -y, -z; (4) x, y, z.			

Table 6S: Complex 5

D-H···A	**H···A (Å)**	**D···A (Å)**	**∠D-H···A (°)**
N7-H7···O1[1]	1.96	2.8001	165
N18-H18···O3[1]	1.99	2.8175	162
N29-H29···O1[1]	2.06	2.8395	150
C15-H15···O1[1]	2.41	3.2750	154
C37-H37···O1[1]	2.43	3.3348	165
C40-H40B···O9[2]	2.48	3.3648	153
C43-H43B···O20[3]	2.54	3.4919	165
C55-H55B···O31[4]	2.31	3.2743	170
C36-H36···O3[5]	2.50	3.4268	174
Symmetry codes: (1) 1-x, 1-y, -z; (2) 2-x, 1-y, 1-z; (3) -1+x, y, z; (4) -1+x, -1+y, z; (5) x, y, z.			

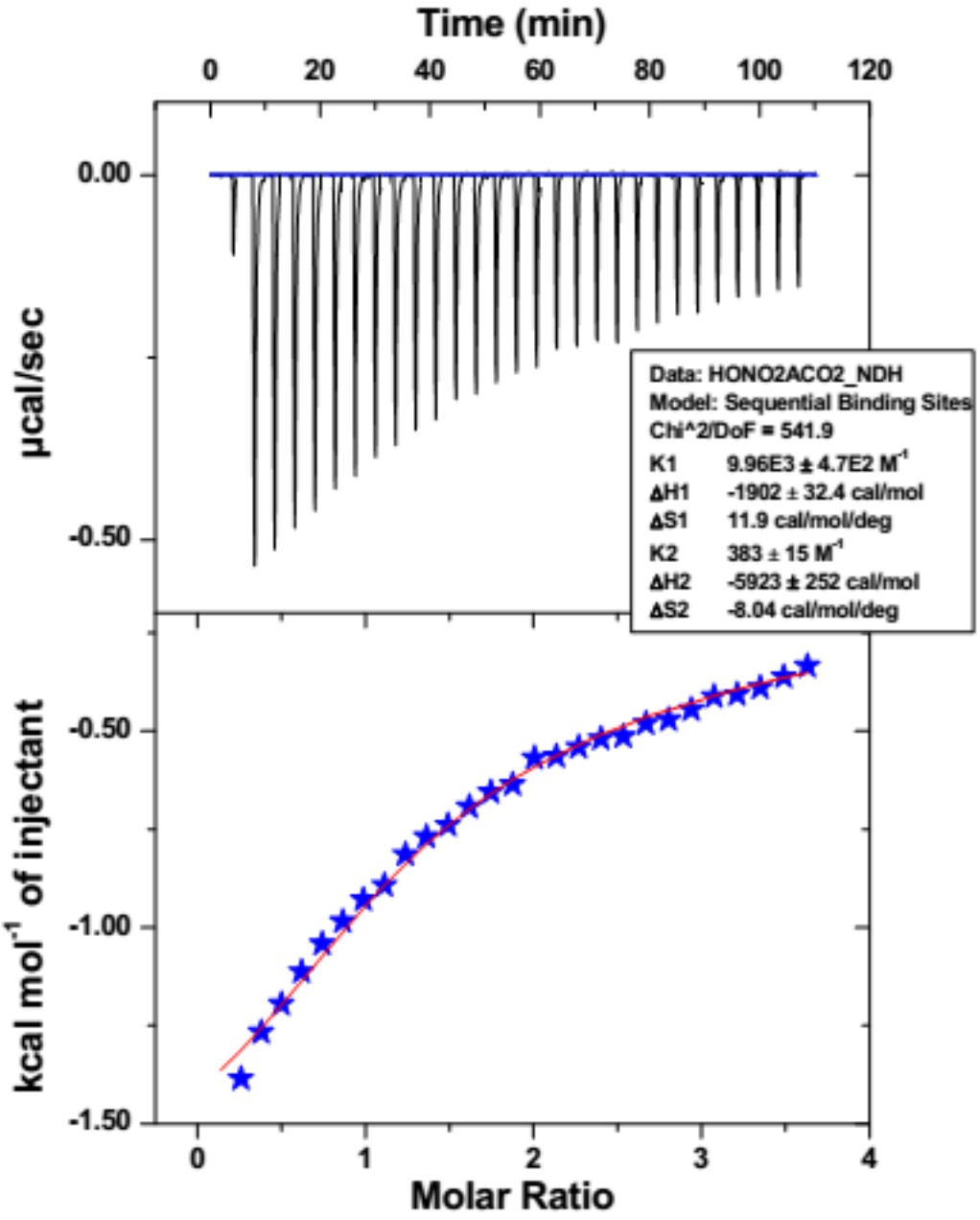

Fig. 27S: ITC titration profile of **L1** to TAcO at 298K. Concentrations maintained during experiment are [**L1**] = 0.276mM, [TAcO] = 4.704mM. Thermodynamic parameters associated with this titration are, K1 = 9.96E3 ± 4.7E2 M^{-1}, ΔH1 = -1902 ± 32.4 cal/mol, ΔS1 = 11.9 cal/mol/deg, K2 = 383 ± 15 M^{-1}, ΔH2 = -5923 ± 252 cal/mol, ΔS2 = -8.04 cal/mol/deg, Chi^2/DOF = 541.9.

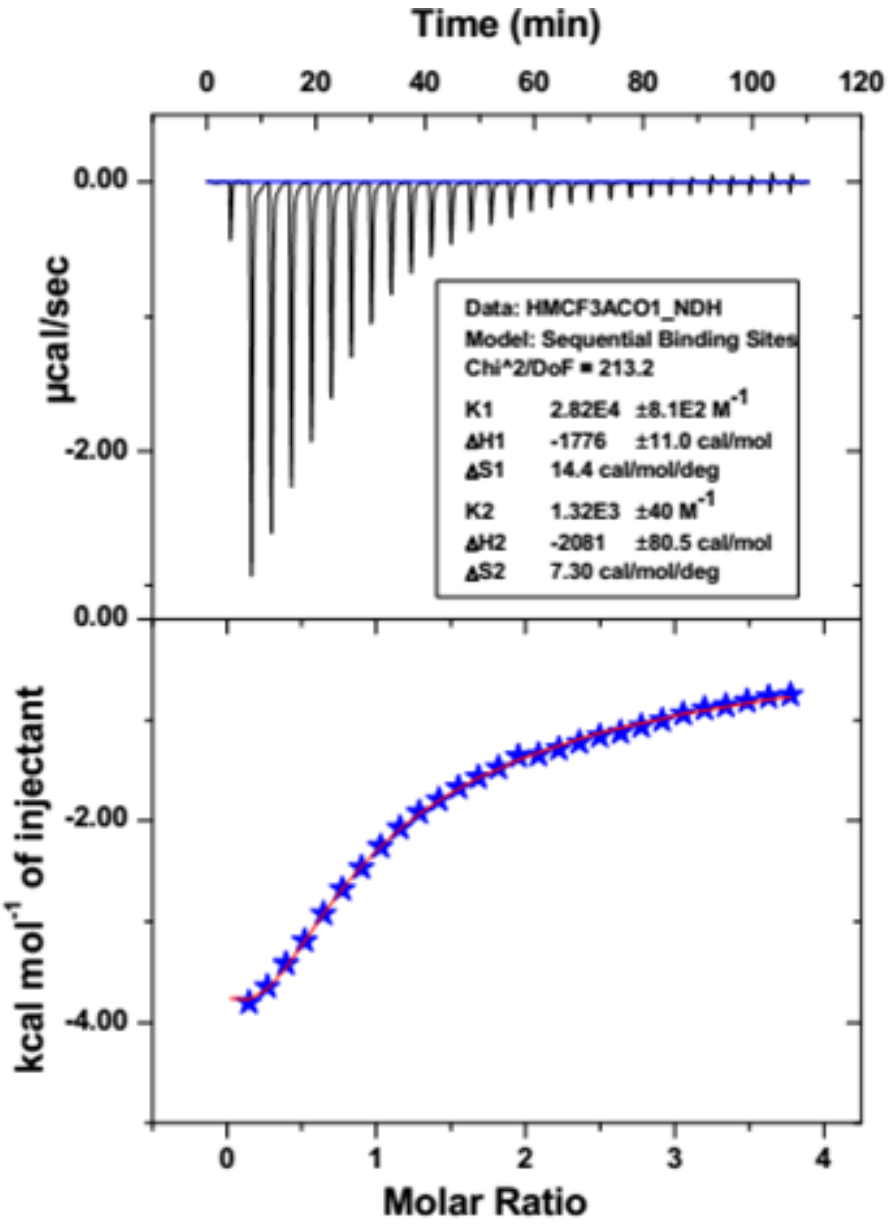

Fig. 28S: ITC titration profile of **L3** to TAcO at 298K. Concentrations maintained during experiment are [**L3**] = 0.2654mM, [TAcO] = 4.704mM. Thermodynamic parameters associated with this titration are, K1 = 2.82E4 ± 8.1E2 M^{-1}, ΔH1 = -1776 ± 11.0 cal/mol, ΔS1 = 14.4 cal/mol/deg, K2 = 1.32E3 ± 40 M^{-1}, ΔH2 = -2081 ± 80.5 cal/mol, ΔS2 = 7.30 cal/mol/deg, Chi^2/DOF = 213.2.

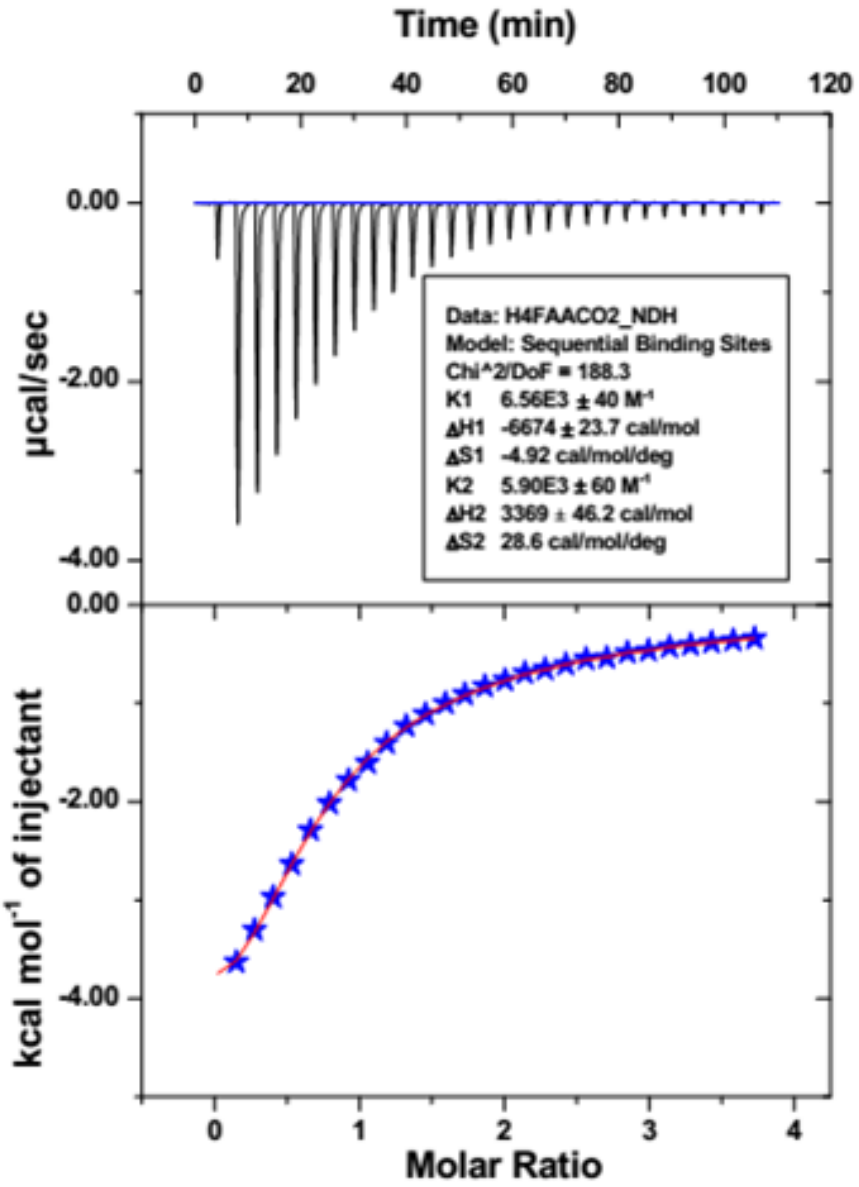

Fig. 29S: ITC titration profile of **L4** to TAcO at 298K. Concentrations maintained during experiment are [**L4**] = 0.2548mM, [TAcO] = 4.704mM. Thermodynamic parameters associated with this titration are, K1 = 6.56E3 ± 40 M^{-1}, ΔH1 = -6674 ± 23.7 cal/mol, ΔS1 = -4.92 cal/mol/deg, K2 = 5.90E3 ± 60 M^{-1}, ΔH2 = 3369 ± 46.2 cal/mol, ΔS2 = 28.6 cal/mol/deg, Chi^2/DOF = 188.3.

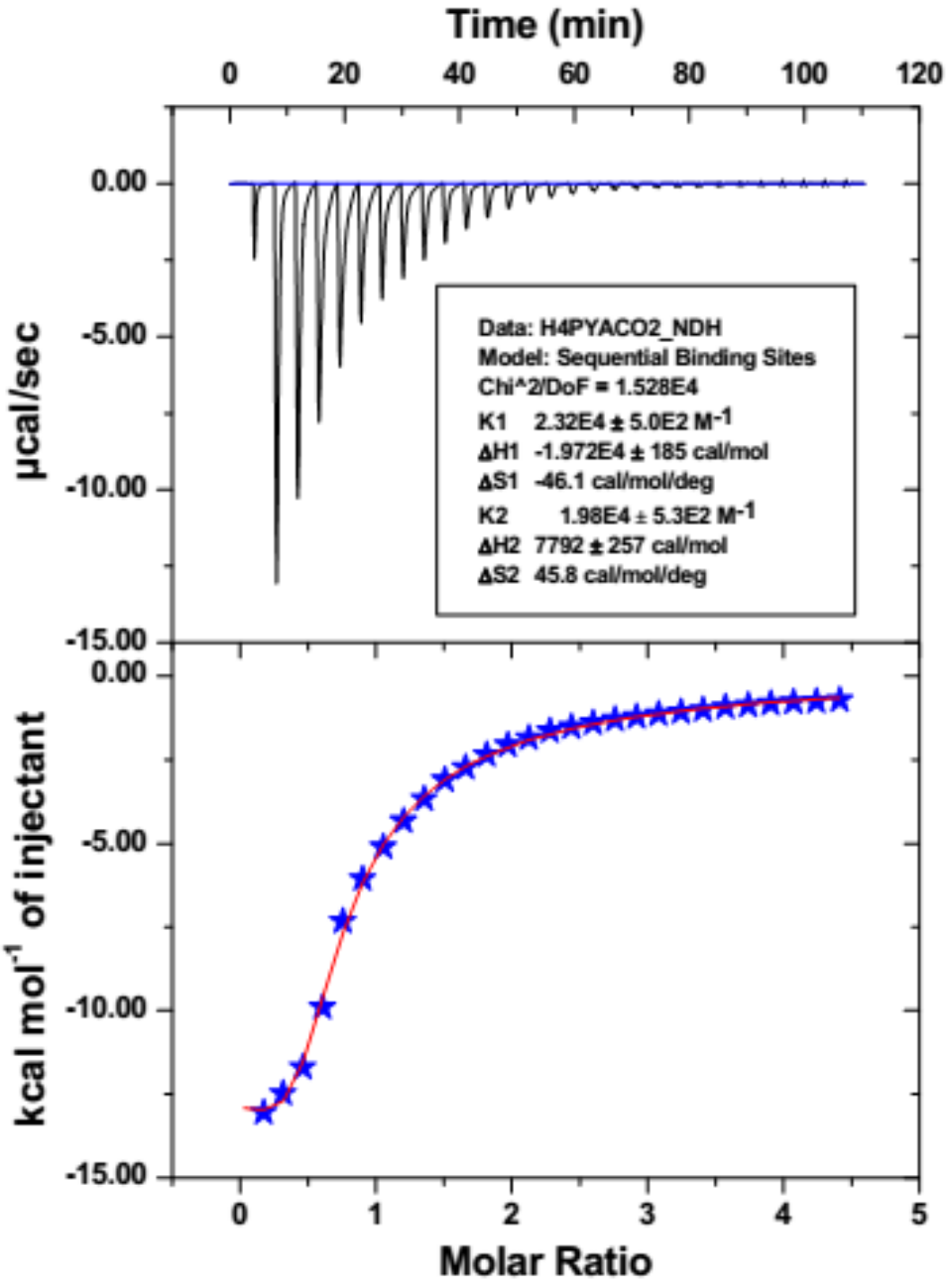

Fig. 30S: ITC titration profile of **L5** to TAcO at 298K. Concentrations maintained during experiment are [**L5**] = 0.227mM, [TAcO] = 4.704mM. Thermodynamic parameters associated with this titration are, K1 = 2.32E4 ± 5.0E2 M^{-1}, ΔH1 = -19720 ± 185 cal/mol, ΔS1 = -46.1 cal/mol/deg, K2 = 1.98E4 ± 5.3E2 M^{-1}, ΔH2 = 7792 ± 257 cal/mol, ΔS2 = 45.8 cal/mol/deg, Chi^2/DOF = 1.528E4.

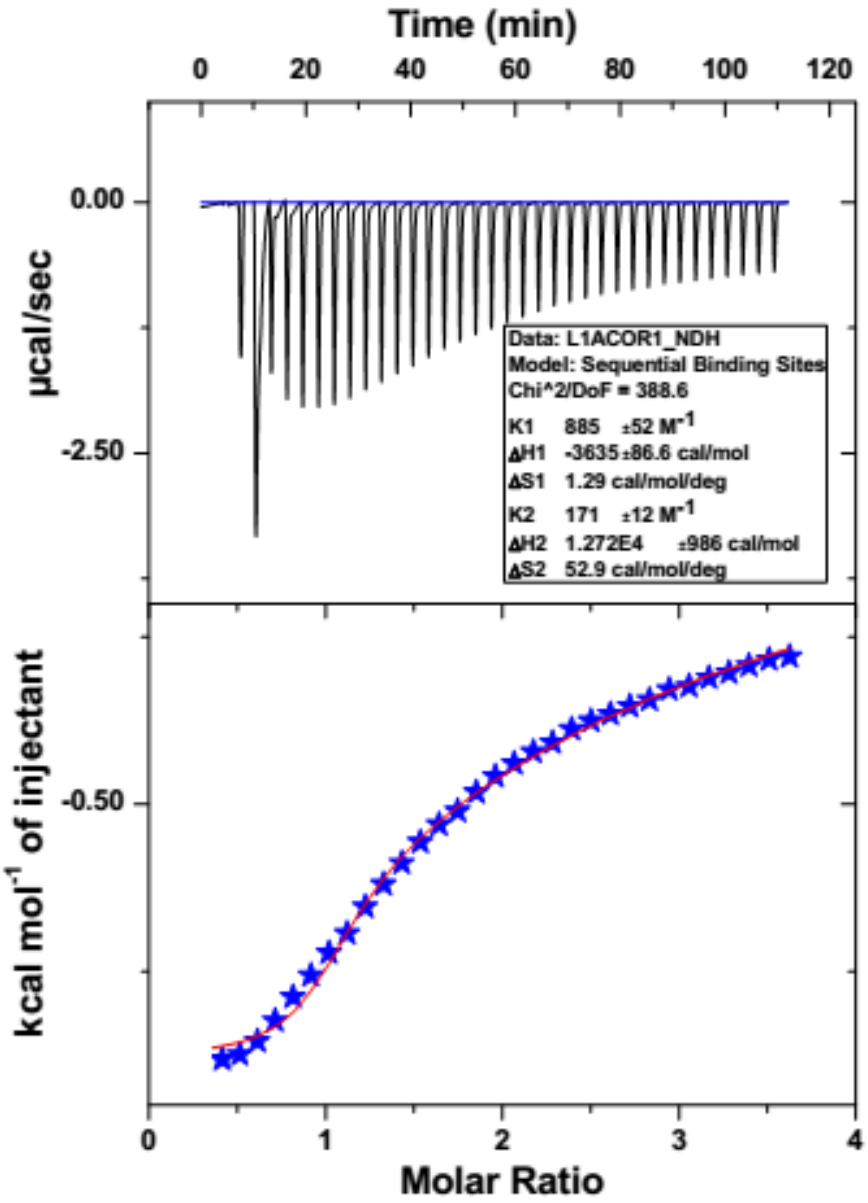

Fig. 31S: ITC titration profile of **L6** to TAcO at 298K. Concentrations maintained during experiment are [**L6**] = 0.239mM, [TAcO] = 4.704mM. Thermodynamic parameters associated with this titration are, K1 = 885 ± 52 M^{-1}, ΔH1 = -3635 ± 86.6 cal/mol, ΔS1 = 1.29 cal/mol/deg, K2 = 171 ± 12 M^{-1}, ΔH2 = 1.272E4 ± 986 cal/mol, ΔS2 = 52.9 cal/mol/deg, Chi^2/DOF = 388.6.

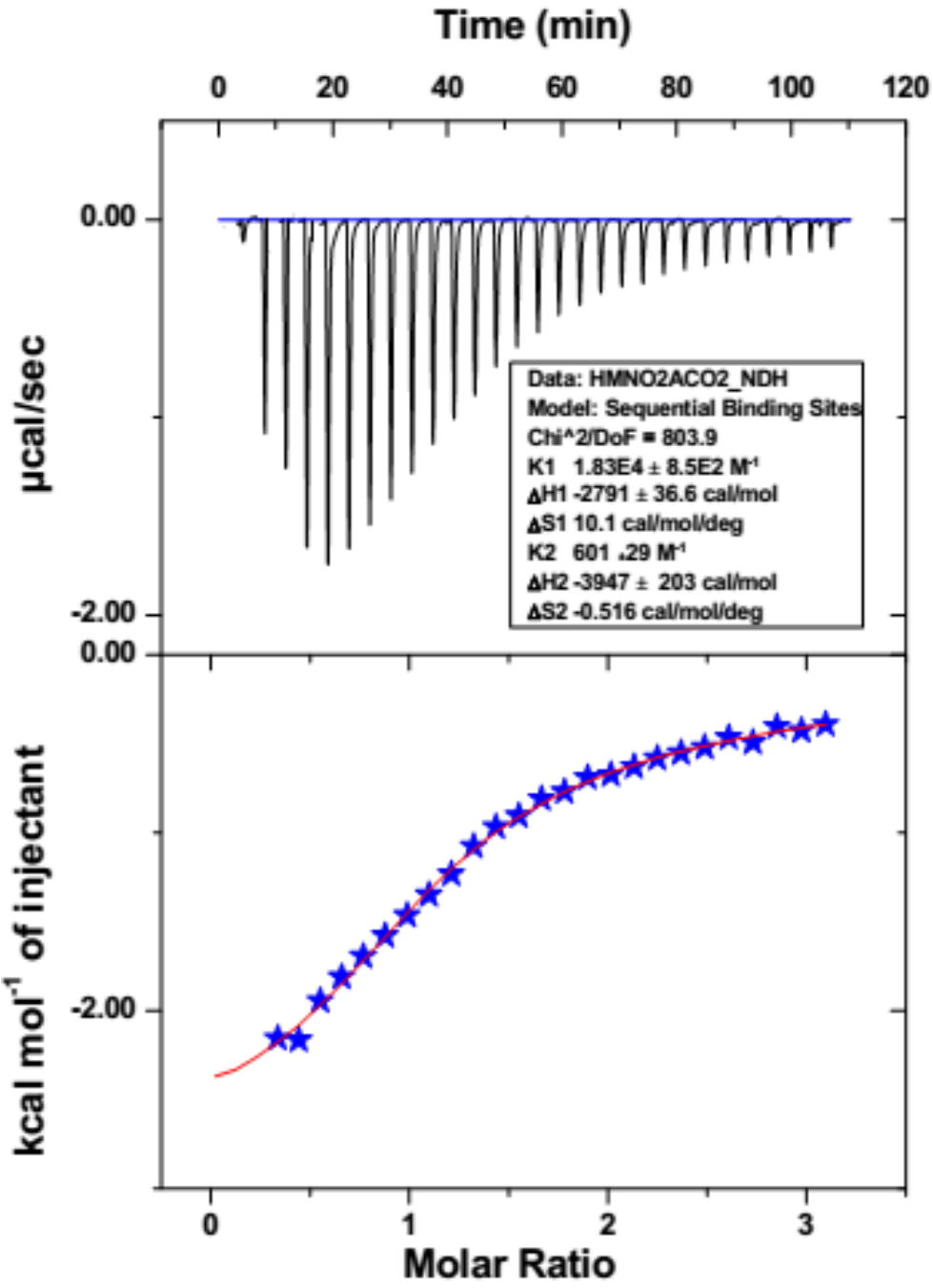

Fig. 32S: ITC titration profile of **L7** to TAcO at 298K. Concentrations maintained during experiment are [**L7**] = 0.311mM, [TAcO] = 4.704mM. Thermodynamic parameters associated with this titration are, K1 = 1.83E4 ± 8.5E2 M^{-1}, ΔH1 = -2791 ± 36.6 cal/mol, ΔS1 = 10.1 cal/mol/deg, K2 = 601 ± 29 M^{-1}, ΔH2 = -3947 ± 203 cal/mol, ΔS2 = -0.516 cal/mol/deg, Chi^2/DOF = 803.9.

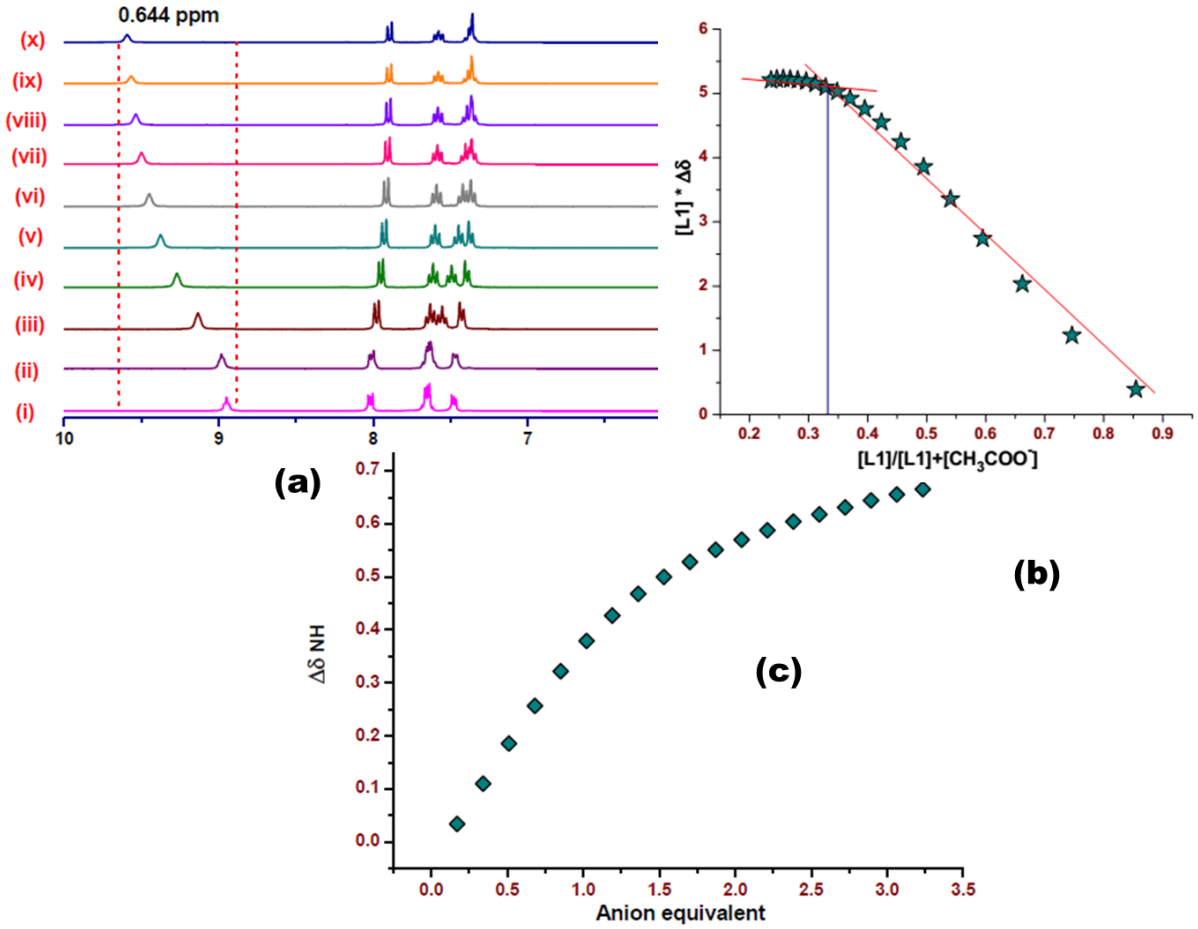

Fig. 33S: (a) Partial ^{1}H-NMR (300 MHz) spectral changes of **L1** in DMSO-d_6 with added AcO^{-} in DMSO-d_6 (298K), [**L1**] = 11.80mM. The respective ratio of concentrations are [AcO^{-}]/[**L1**]: (i) 0, (ii) 0.17, (iii) 0.51, (iv) 0.85, (v) 1.19, (vi) 1.53, (vii) 1.87, (viii) 2.21, (ix) 2.55, (x) 2.89. (b) Molar ratio plot of titration for **L1** with AcO^{-} in DMSO-d_6 which shows a 1:2 stoichiometry. (c) Anion equivalent plot for titration of **L1** with AcO^{-}.

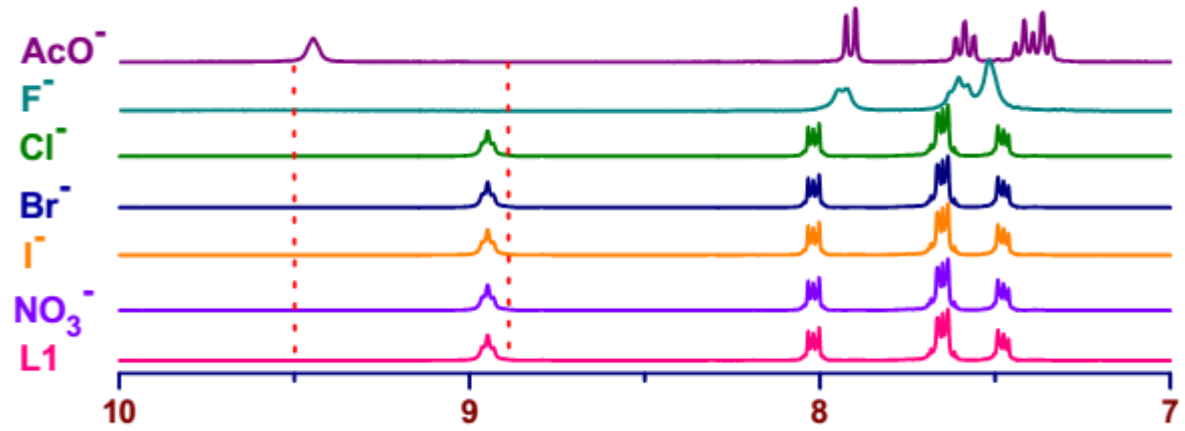

Fig. 34S: Comparative partial ^{1}H NMR (300 MHz) spectra of **L1** (~ 5 mM) in DMSO-d_6 after addition of excess amount (~1 equivalent) of TBA salts of different anions.

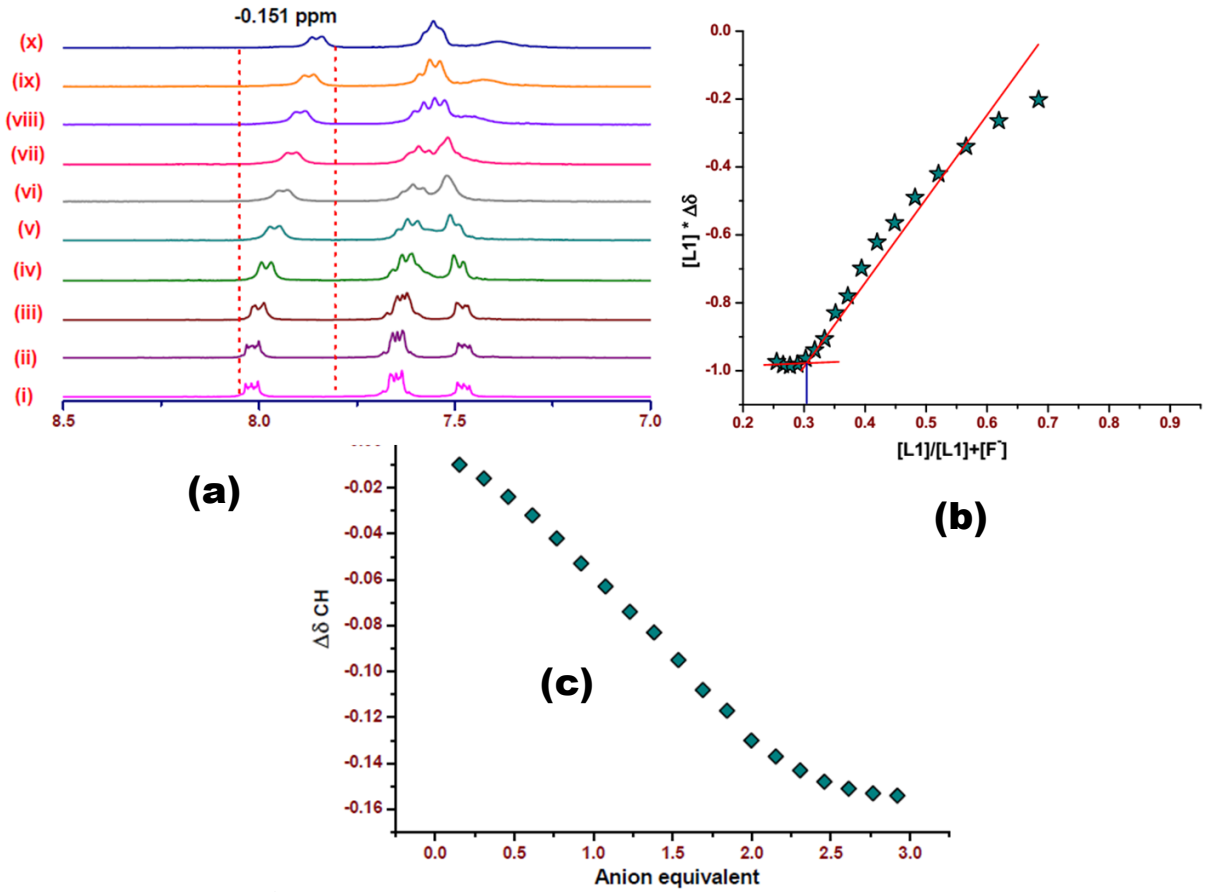

Fig. 35S: (a) Partial ^{1}H-NMR (300 MHz) spectral changes of **L1** in DMSO-d_6 with added F^{-} in DMSO-d_6 (298K), [**L1**] = 8.98mM. The respective ratio of concentrations are [F^{-}]/[**L1**]: (i) 0, (ii) 0.15, (iii) 0.46, (iv) 0.76, (v) 1.07, (vi) 1.38, (vii) 1.69, (viii) 1.99, (ix) 2.30, (x) 2.61. (b) Molar ratio plot of titration for **L1** with F^{-} in DMSO-d_6 which shows a 1:2 stoichiometry. (c) Anion equivalent plot for titration of **L1** with F^{-}.

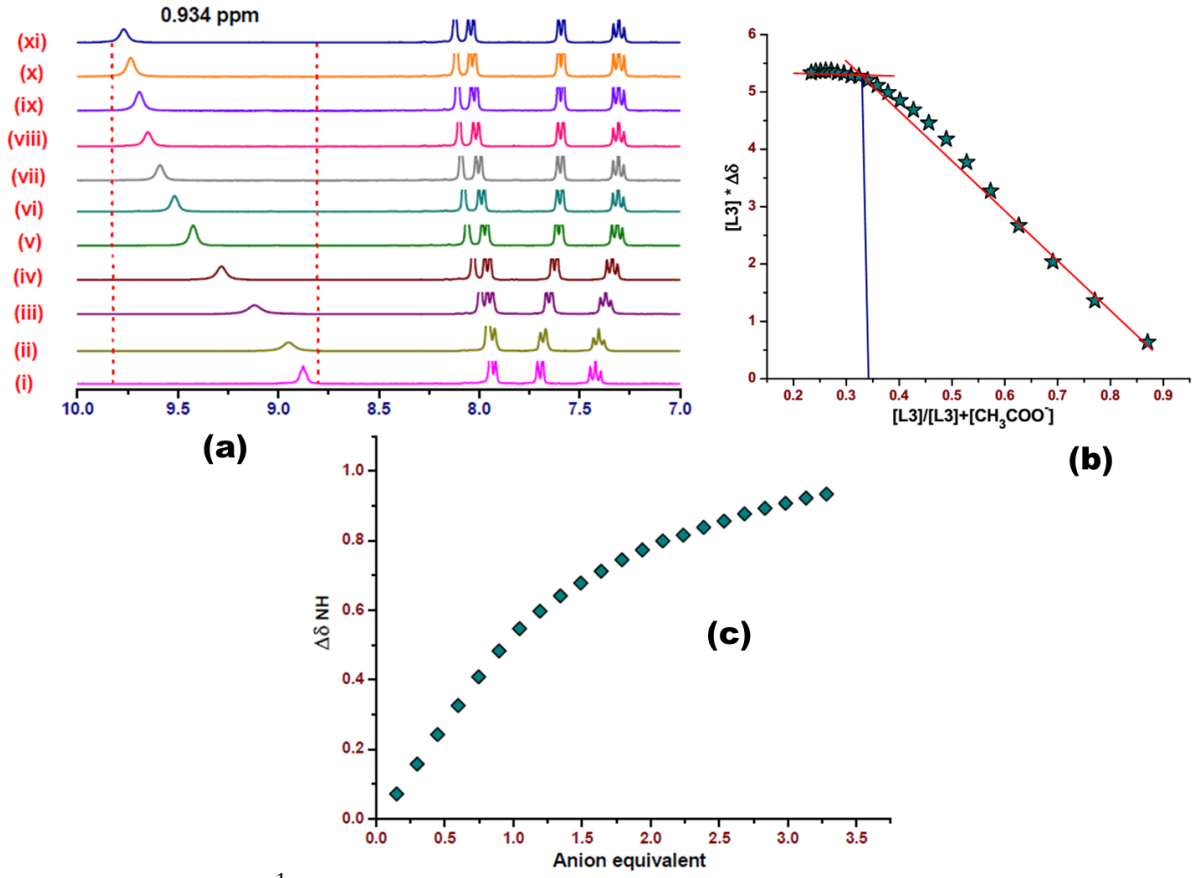

Fig. 36S: (a) Partial ^{1}H-NMR (300 MHz) spectral changes of **L3** in DMSO-d_6 with added AcO^{-} in DMSO-d_6 (298K), [**L3**] = 9.06mM. The respective ratio of concentrations are [AcO^{-}]/[**L3**]: (i) 0, (ii) 0.15, (iii) 0.45, (iv) 0.74, (v) 1.04, (vi) 1.34, (vii) 1.64, (viii) 1.94, (ix) 2.24, (x) 2.54, (xi) 2.83, (xii) 3.13. (b) Molar ratio plot of titration for **L3** with AcO^{-} in DMSO-d_6 which shows a 1:2 stoichiometry. (c) Anion equivalent plot for titration of **L3** with AcO^{-}.

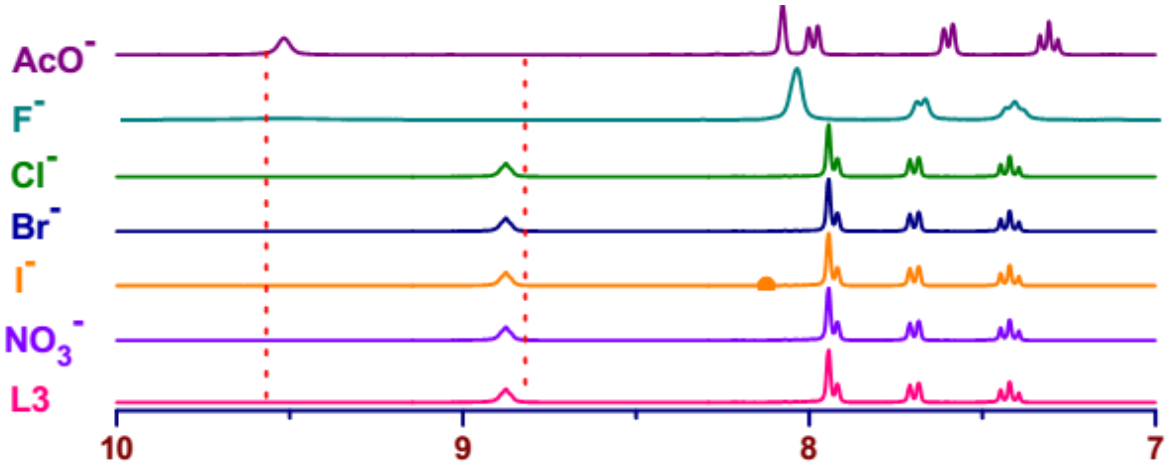

Fig. 37S: Comparative partial ^{1}H NMR (300 MHz) spectra of **L3** (~ 4 mM) in DMSO-d_6 after addition of excess amount (~1 equivalent) of TBA salts of different anions.

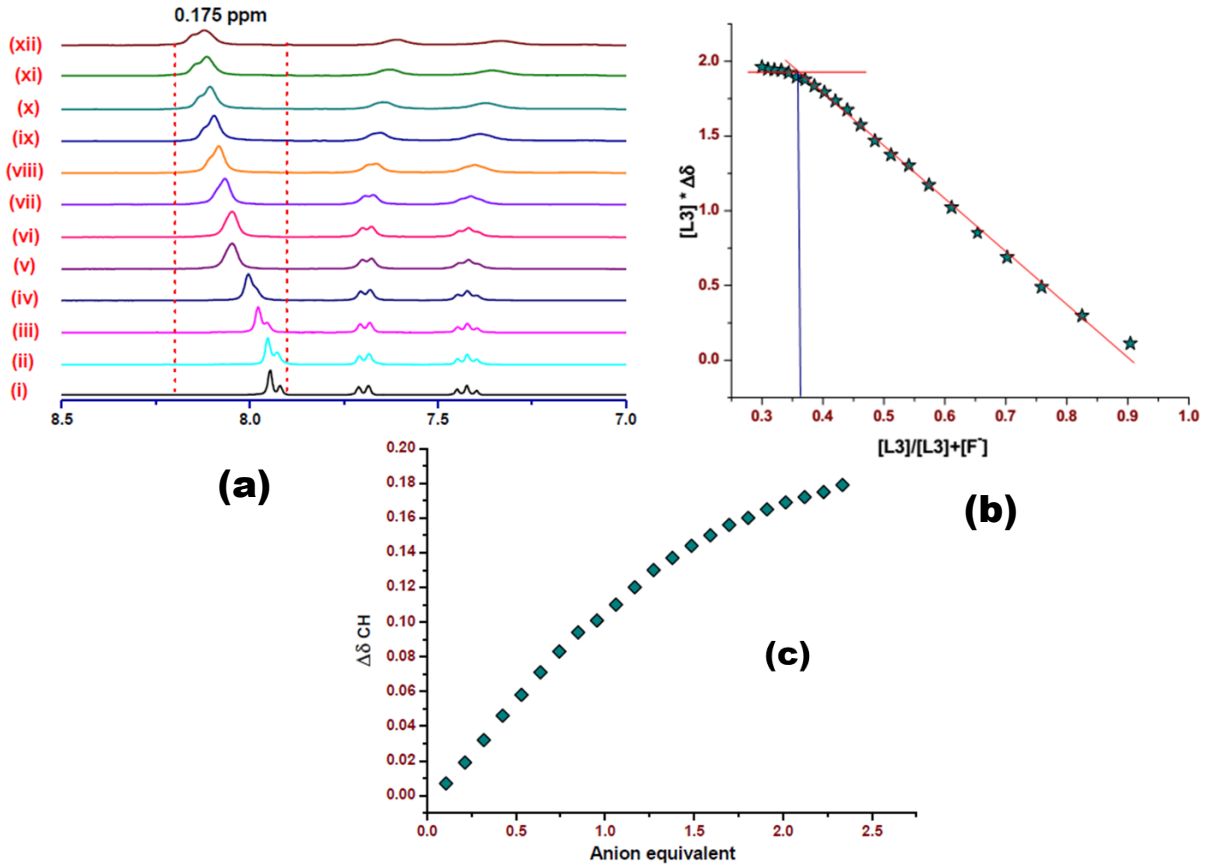

Fig. 38S: (a) Partial ^{1}H-NMR (300 MHz) spectral changes of **L3** in DMSO-d_6 with added F^- in DMSO-d_6 (298K), [**L3**] = 12.32mM. The respective ratio of concentrations are [F^-]/[**L3**]: (i) 0, (ii) 0.11, (iii) 0.32, (iv) 0.53, (v) 0.74, (vi) 1.16, (vii) 1.48, (viii) 1.692, (ix) 1.90, (x) 2.23, (xi) 2.55. (b) Molar ratio plot of titration for **L3** with F^- in DMSO-d_6 which shows a 1:2 stoichiometry. (c) Anion equivalent plot for titration of **L3** with F^-.

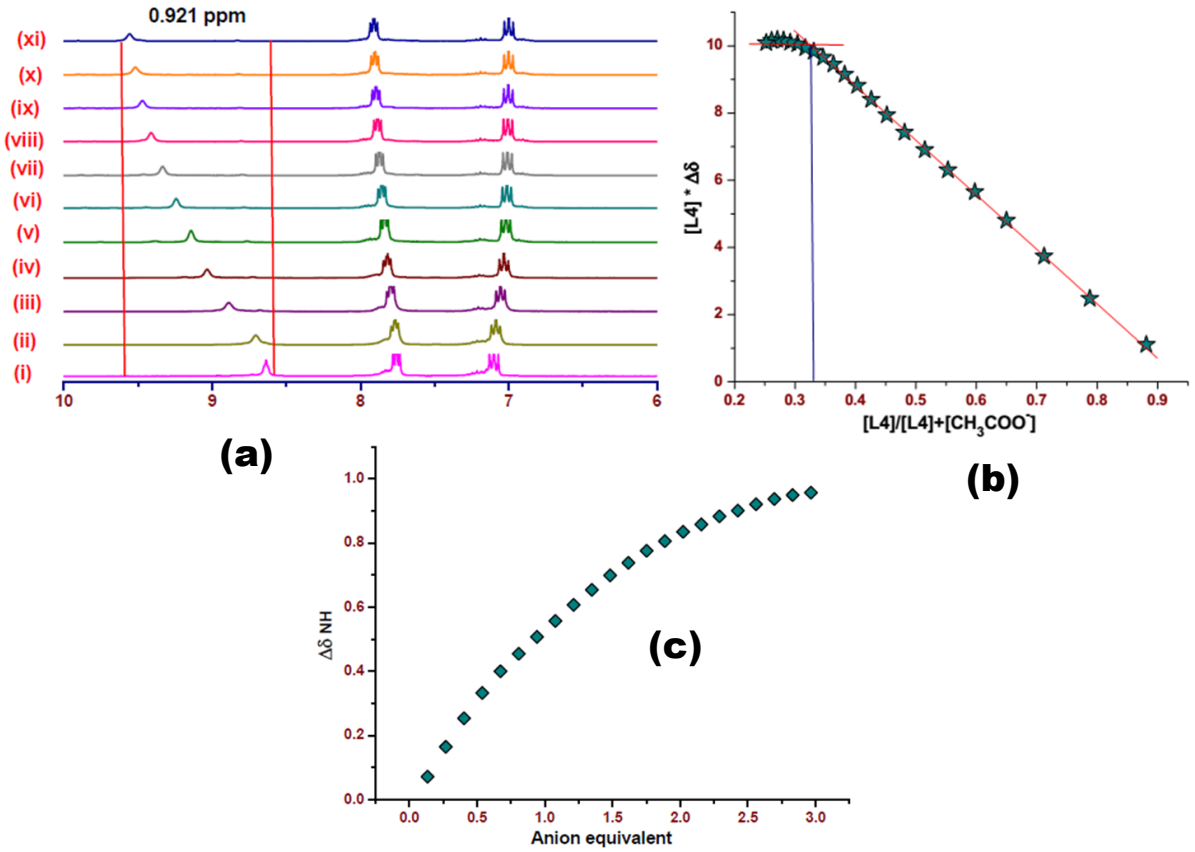

Fig. 39S: (a) Partial ^{1}H-NMR (300 MHz) spectral changes of **L4** in DMSO-d_6 with added AcO^- in DMSO-d_6 (298K), [**L4**] = 10.70mM. The respective ratio of concentrations are [AcO^-]/[**L4**]: (i) 0, (ii) 0.13, (iii) 0.40, (iv) 0.67, (v) 0.94, (vi) 1.21, (vii) 1.48, (viii) 1.75, (ix) 2.02, (x) 2.29, (xi) 2.56. (b) Molar ratio plot of titration for **L4** with AcO^- in DMSO-d_6 which shows a 1:2 stoichiometry. (c) Anion equivalent plot for titration of **L4** with AcO^-.

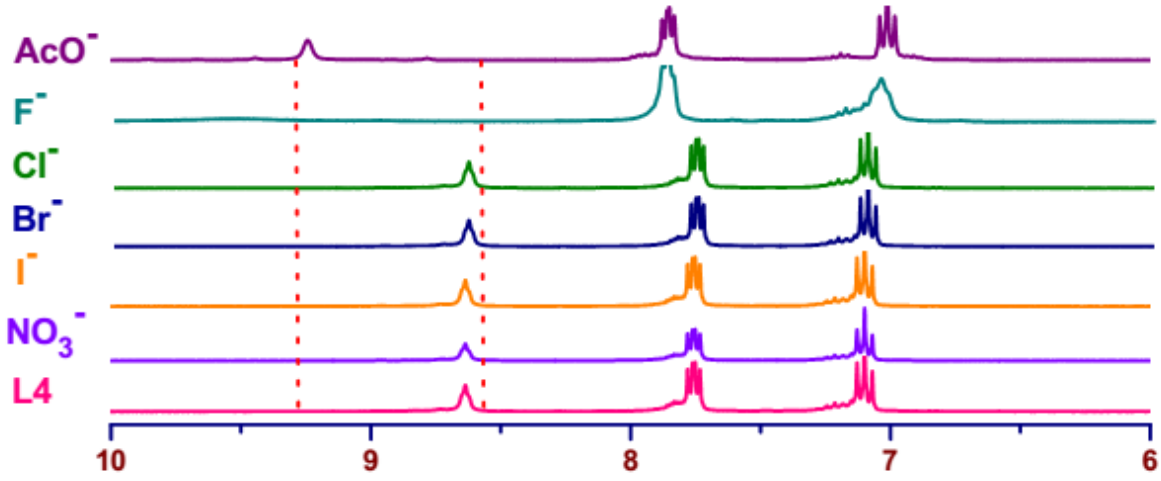

Fig. 40S: Comparative partial ^{1}H NMR (300 MHz) spectra of **L4** (~ 5 mM) in DMSO-d_6 after addition of excess amount (~1 equivalent) of TBA salts of different anions.

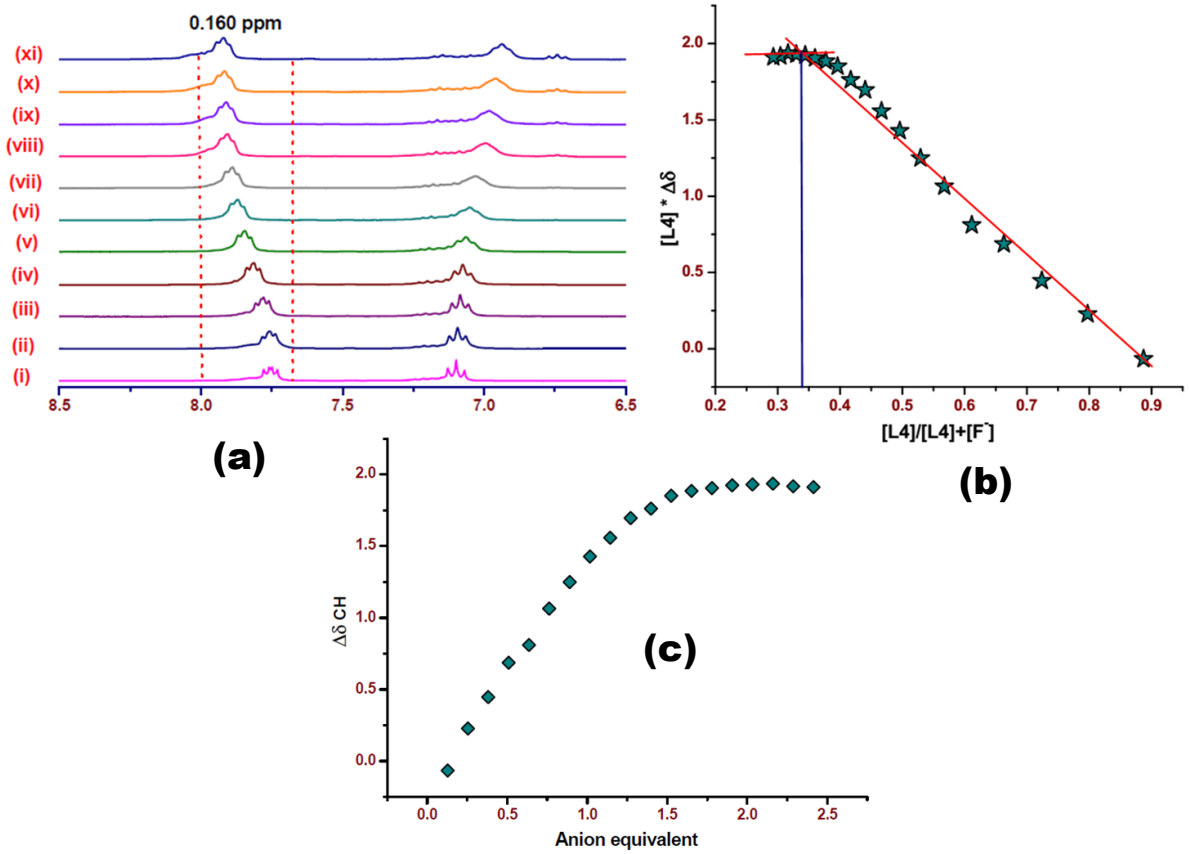

Fig. 41S: (a) Partial ^{1}H-NMR (300 MHz) spectral changes of **L4** in DMSO-d_6 with added F^- in DMSO-d_6 (298K), [**L4**] = 11.15mM. The respective ratio of concentrations are [F^-]/[**L4**]: (i) 0, (ii) 0.12, (iii) 0.38, (iv) 0.64, (v) 0.89, (vi) 1.14, (vii) 1.40, (viii) 1.65, (ix) 1.91, (x) 2.16, (xi) 2.41. (b) Molar ratio plot of titration for **L4** with F^- in DMSO-d_6 which shows a 1:2 stoichiometry. (c) Anion equivalent plot for titration of **L4** with F^-.

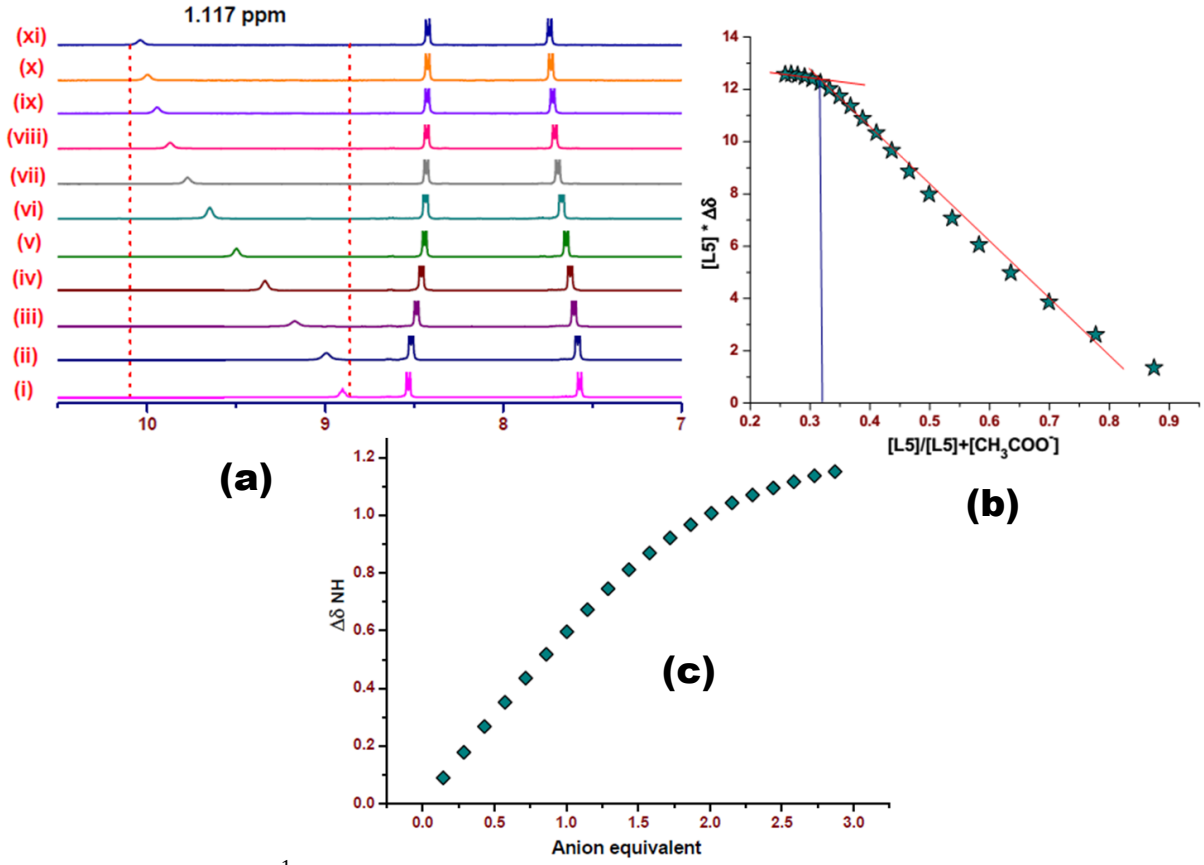

Fig. 42S: (a) Partial ^{1}H-NMR (300 MHz) spectral changes of **L5** in DMSO-d_6 with added AcO^{-} in DMSO-d_6 (298K), [**L5**] = 15.28mM. The respective ratio of concentrations are [AcO^{-}]/[**L5**]: (i) 0, (ii) 0.14, (iii) 0.43, (iv) 0.72, (v) 1.00, (vi) 1.29, (vii) 1.58, (viii) 1.87, (ix) 2.15, (x) 2.44, (xi) 2.73. (b) Molar ratio plot of titration for **L5** with AcO^{-} in DMSO-d_6 which shows a 1:2 stoichiometry. (c) Anion equivalent plot for titration of **L5** with AcO^{-}.

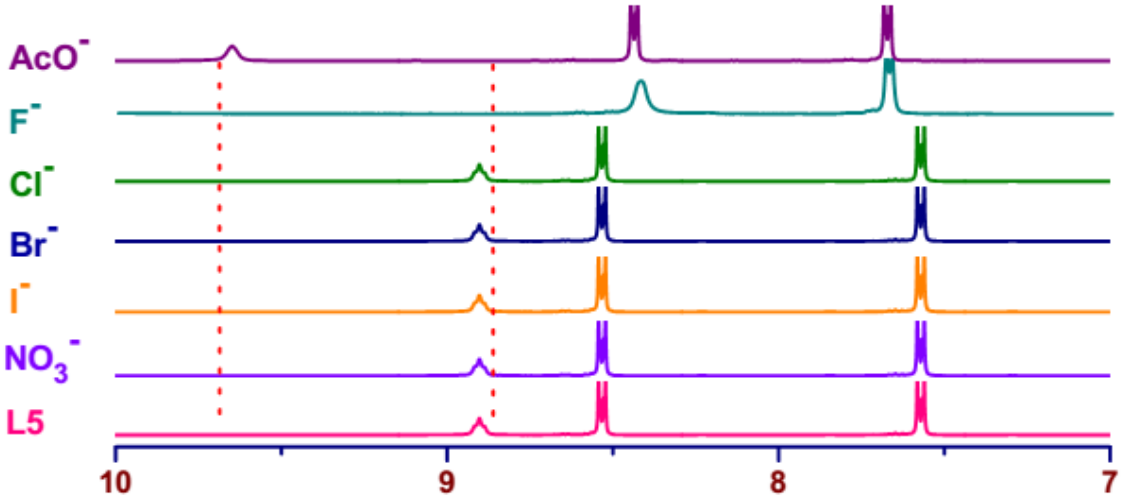

Fig. 43S: Comparative partial ^{1}H NMR (300 MHz) spectra of **L5** (~ 6 mM) in DMSO-d_6 after addition of excess amount (~1 equivalent) of TBA salts of different anions.

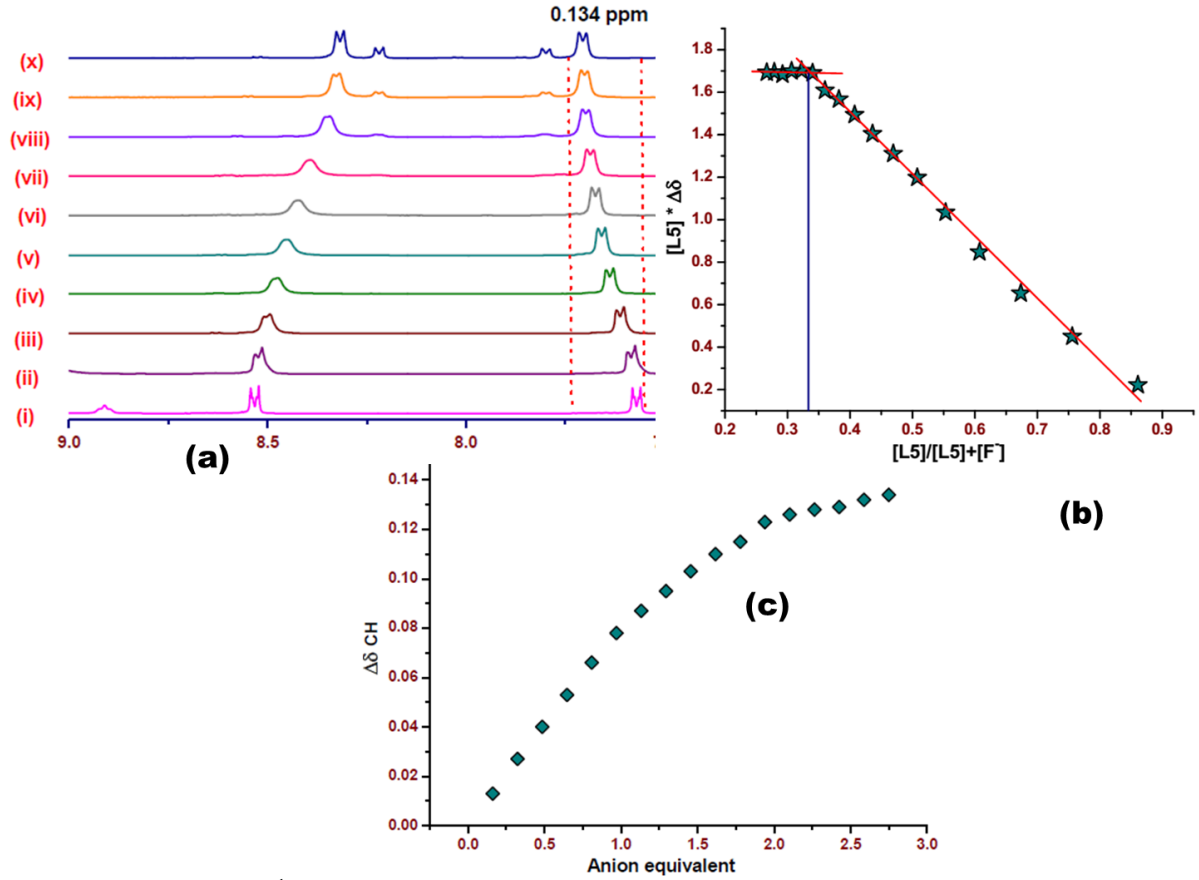

Fig. 44S: (a) Partial ^{1}H-NMR (300 MHz) spectral changes of **L5** in DMSO-d_6 with added AcO^{-} in DMSO-d_6 (298K), [**L5**] = 15.35mM. The respective ratio of concentrations are [AcO^{-}]/[**L5**]: (i) 0, (ii) 0.16, (iii) 0.48, (iv) 0.80, (v) 1.13, (vi) 1.45, (vii) 1.78, (viii) 2.10, (ix) 2.42, (x) 2.74, (xi) 3.06. (b) Molar ratio plot of titration for **L5** with AcO^{-} in DMSO-d_6 which shows a 1:2 stoichiometry. (c) Anion equivalent plot for titration of **L5** with AcO^{-}.

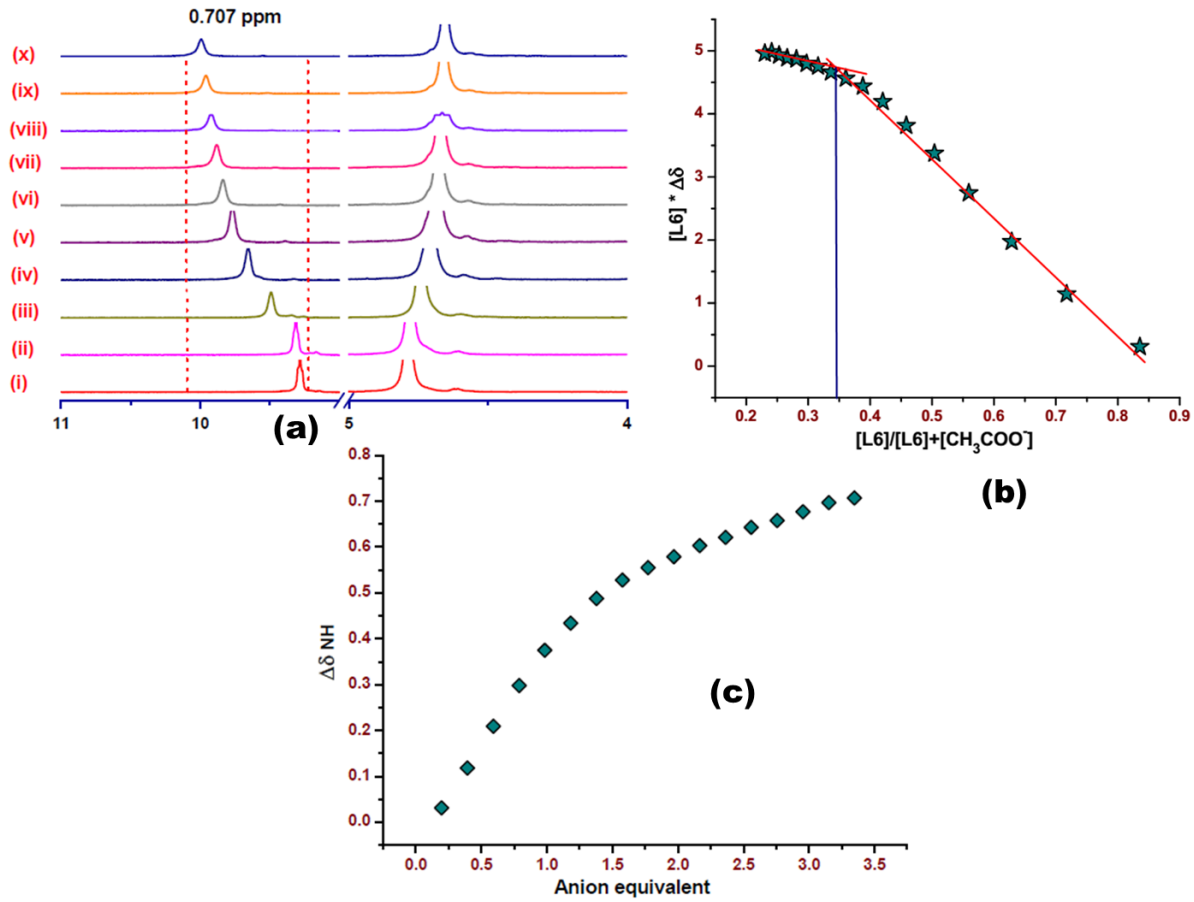

Fig. 45S: (a) Partial ^{1}H-NMR (300 MHz) spectral changes of **L6** in DMSO-d_6 with added AcO^- in DMSO-d_6 (298K), [**L6**] = 10.19mM. The respective ratio of concentrations are [AcO^-]/[**L6**]: (i) 0, (ii) 0.20, (iii) 0.39, (iv) 0.98, (v) 1.38, (vi) 1.77, (vii) 2.16, (viii) 2.56, (ix) 2.95, (x) 3.34. (b) Molar ratio plot of titration for **L6** with AcO^- in DMSO-d_6 which shows a 1:2 stoichiometry. (c) Anion equivalent plot for titration of **L6** with AcO^-.

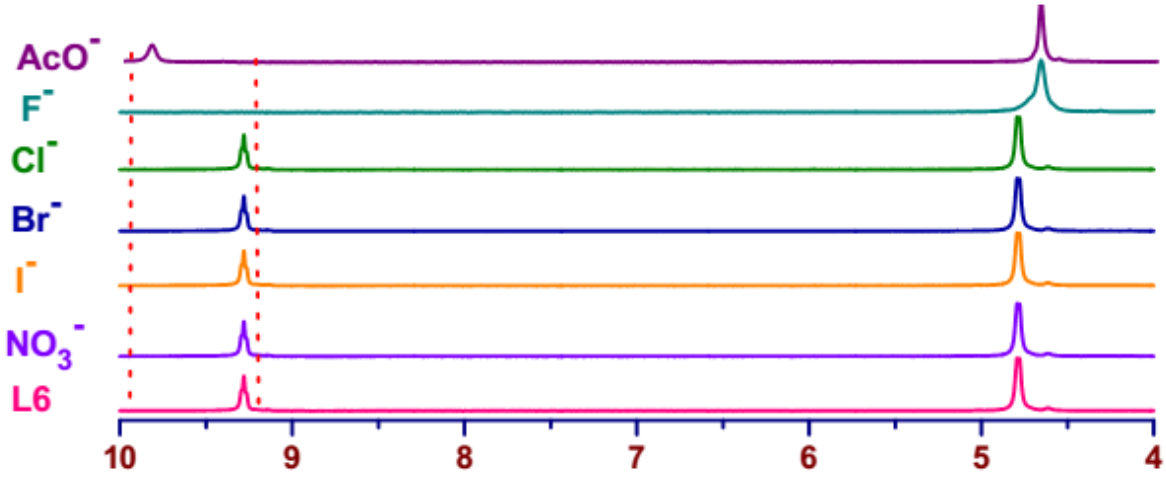

Fig. 46S: Comparative partial ^{1}H NMR (300 MHz) spectra of **L6** (~ 5 mM) in DMSO-d_6 after addition of excess amount (~1 equivalent) of TBA salts of different anions.

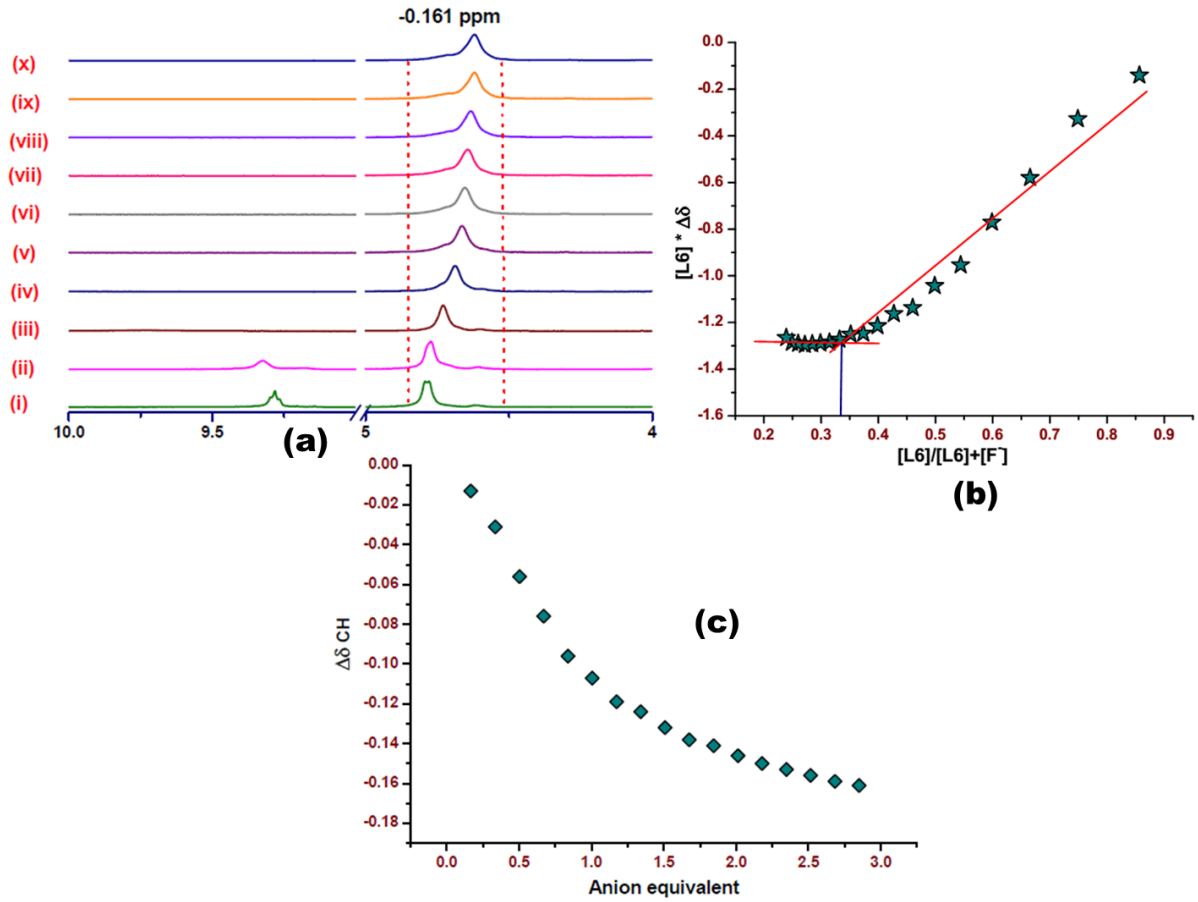

Fig. 47S: (a) Partial ^{1}H-NMR (300 MHz) spectral changes of **L6** in DMSO-d_6 with added F^- in DMSO-d_6 (298K), [**L6**] = 11.04mM. The respective ratio of concentrations are [F^-]/[**L6**]: (i) 0, (ii) 0.17, (iii) 0.50, (iv) 0.84, (v) 1.17, (vi) 1.51, (vii) 1.84, (viii) 2.18, (ix) 2.51, (x) 2.85. (b) Molar ratio plot of titration for **L6** with F^- in DMSO-d_6 which shows a 1:2 stoichiometry.(c) Anion equivalent plot for titration of **L6** with F^-.

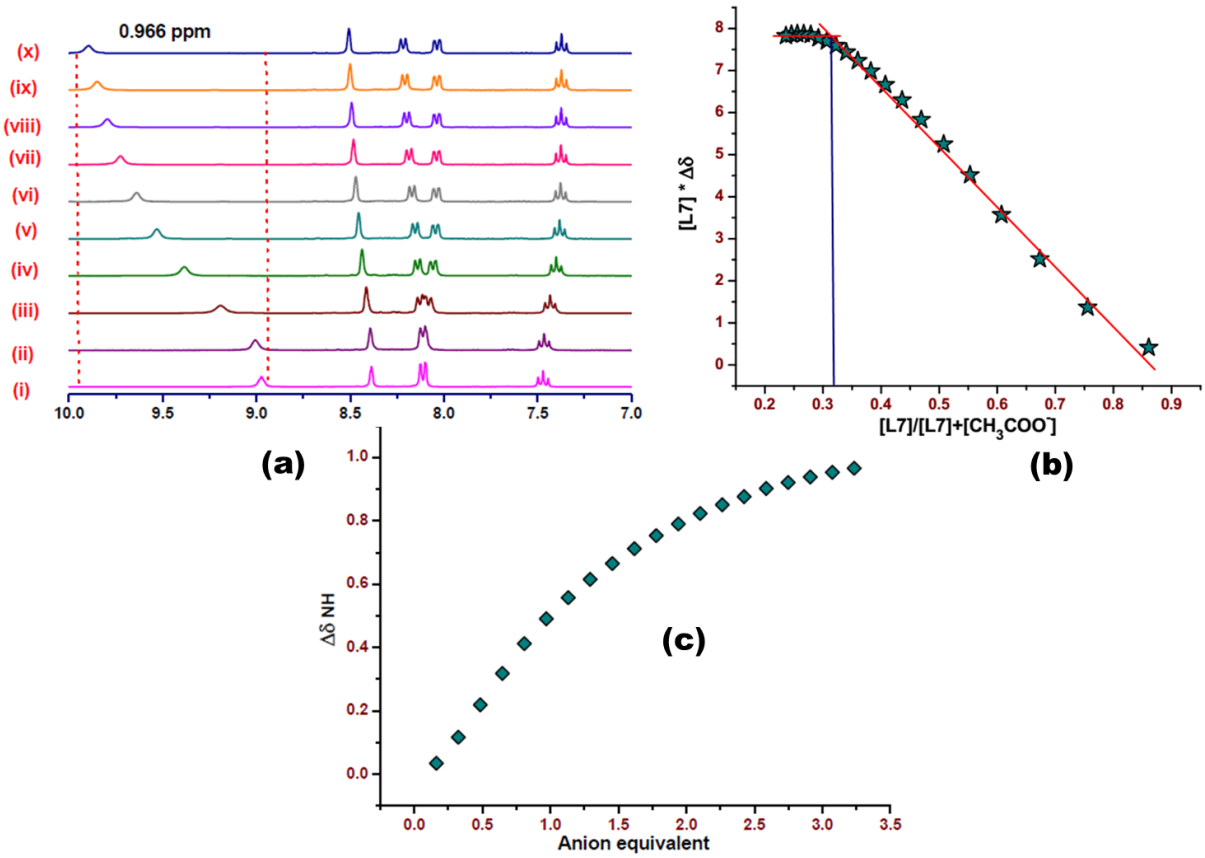

Fig. 48S: (a) Partial ^{1}H-NMR (300 MHz) spectral changes of **L7** in DMSO-d_6 with added AcO^{-} in DMSO-d_6 (298K), [**L7**] = 12.42mM. The respective ratio of concentrations are [AcO^{-}]/[**L7**]: (i) 0, (ii) 0.16, (iii) 0.48, (iv) 0.80, (v) 1.13, (vi) 1.45, (vii) 1.78, (viii) 2.10, (ix) 2.42, (x) 2.75. (b) Molar ratio plot of titration for **L7** with AcO^{-} in DMSO-d_6. which shows a 1:2 stoichiometry. (c) Anion equivalent plot for titration of **L7** with AcO^{-}.

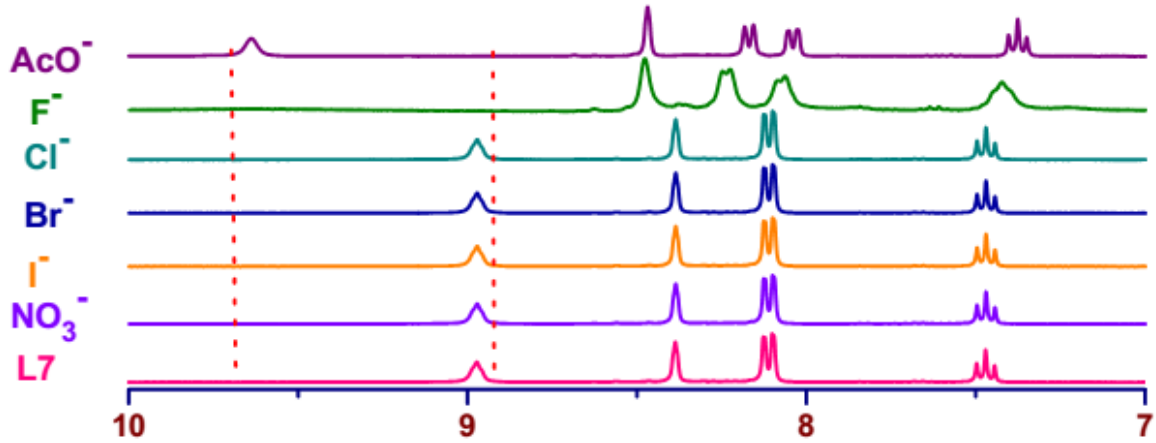

Fig. 49S: Comparative partial ^{1}H NMR (300 MHz) spectra of **L7** (~ 5 mM) in DMSO-d_6 after addition of excess amount (~1 equivalent) of TBA salts of different anions.

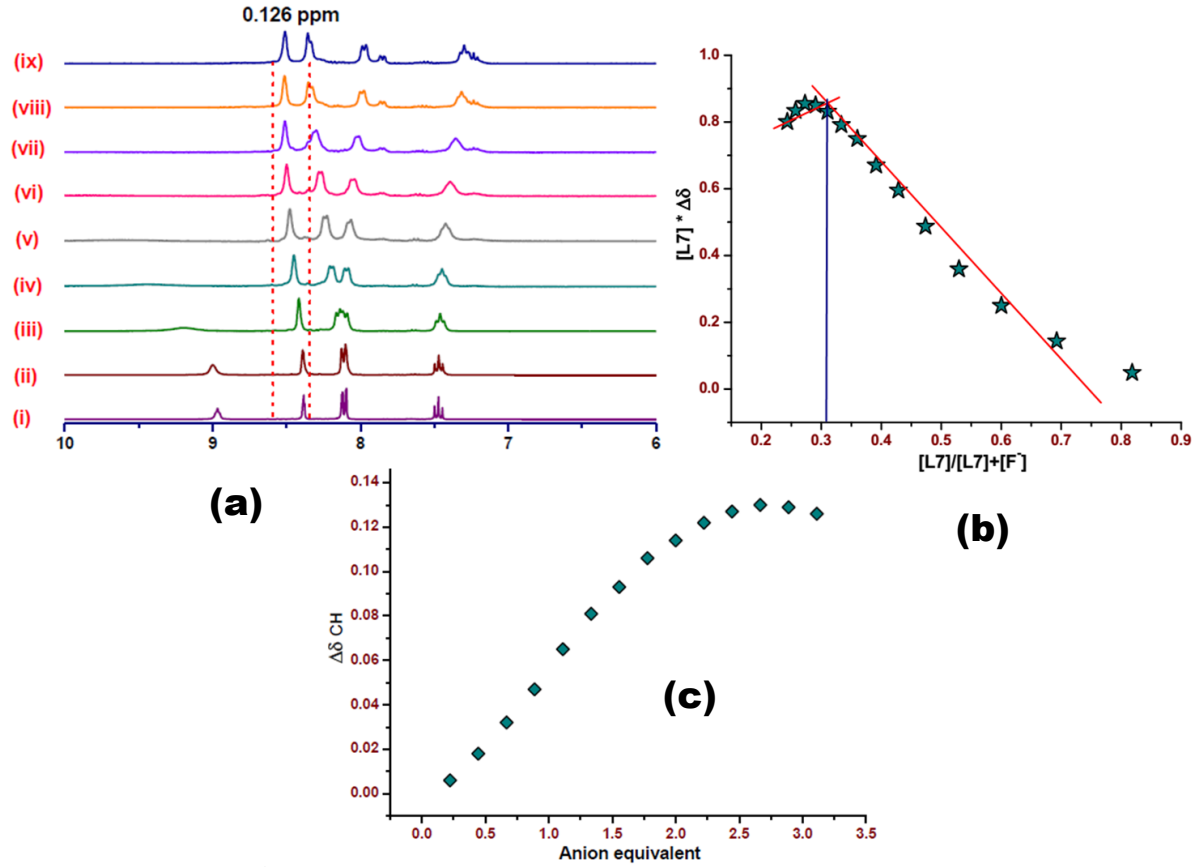

Fig. 50S: (a) Partial ^{1}H-NMR (300 MHz) spectral changes of **L7** in DMSO-d_6 with added F^{-} in DMSO-d_6 (298K), [**L7**] = 8.33mM. The respective ratio of concentrations are [F^{-}]/[**L7**]: (i) 0, (ii) 0.22, (iii) 0.66, (iv) 1.11, (v) 1.56, (vi) 1.99, (vii) 2.44, (viii) 2.88, (ix) 3.11. (b) Molar ratio plot of titration for **L7** with F^{-} in DMSO-d_6 which shows a 1:2 stoichiometry. (c) Anion equivalent plot for titration of **L7** with F^{-}.

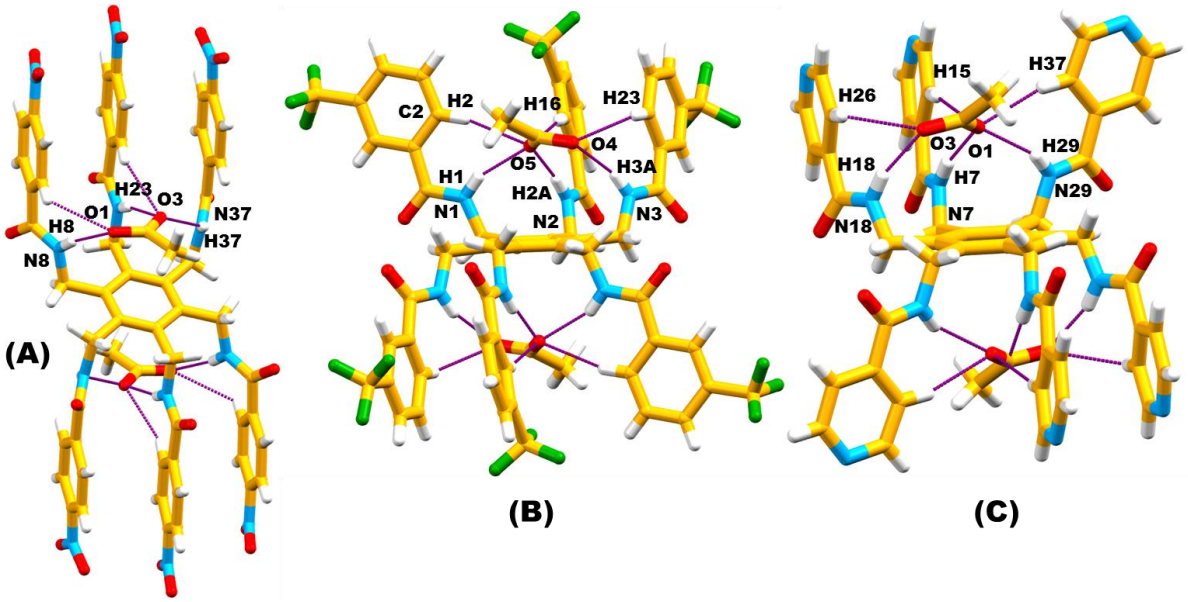

Fig. 51S. Single crystal X-ray structures of (A) complex **3**, (B) complex **4** and (C) complex **5** which showed compartmental recognition of AcO^{-} in ***A*** conformation.

Fig. 52S: Rsidual plot of titration of **L1** vs. AcO^{-} in DMSO-d_6 at 298K.

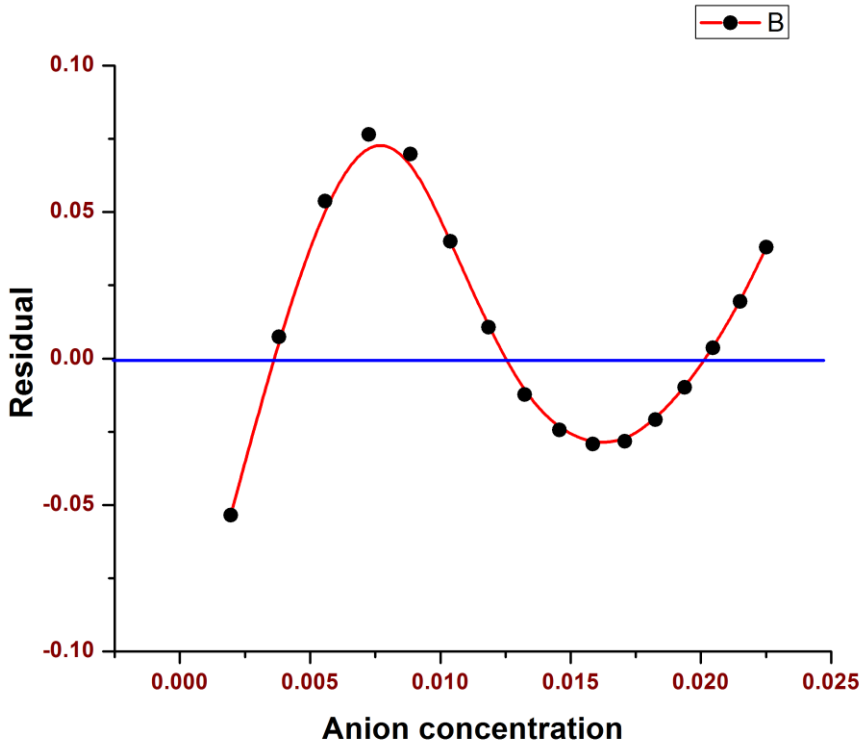

Fig. 53S: Residual plot of titration of **L1** *vs*. F^{-} in DMSO-d_6 at 298K.

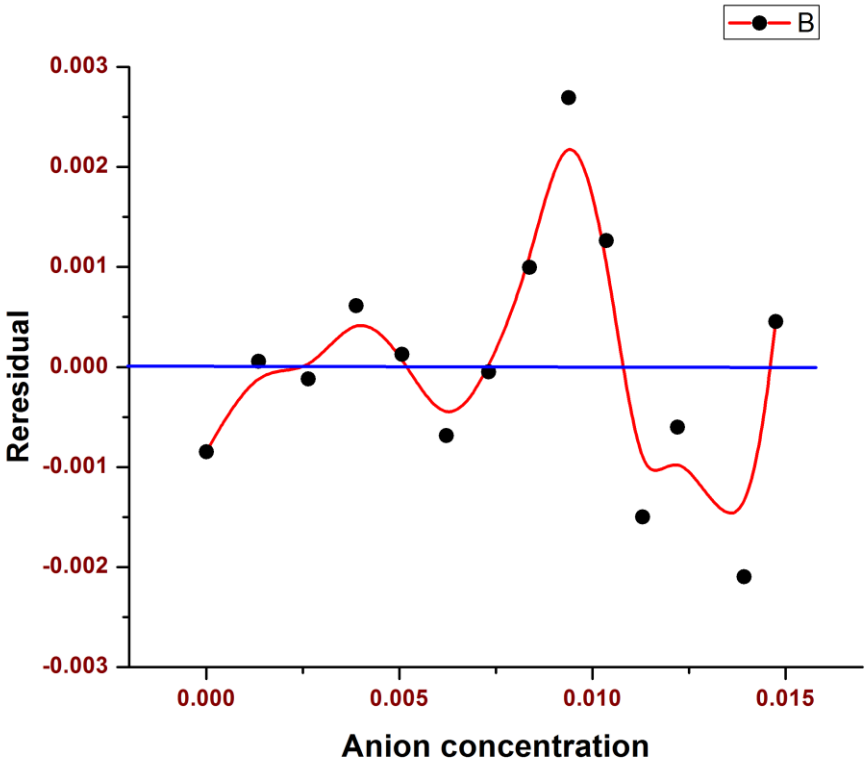

Fig. 54S: Residual plot of titration of **L3** vs. AcO^{-} in DMSO-d_6 at 298K.

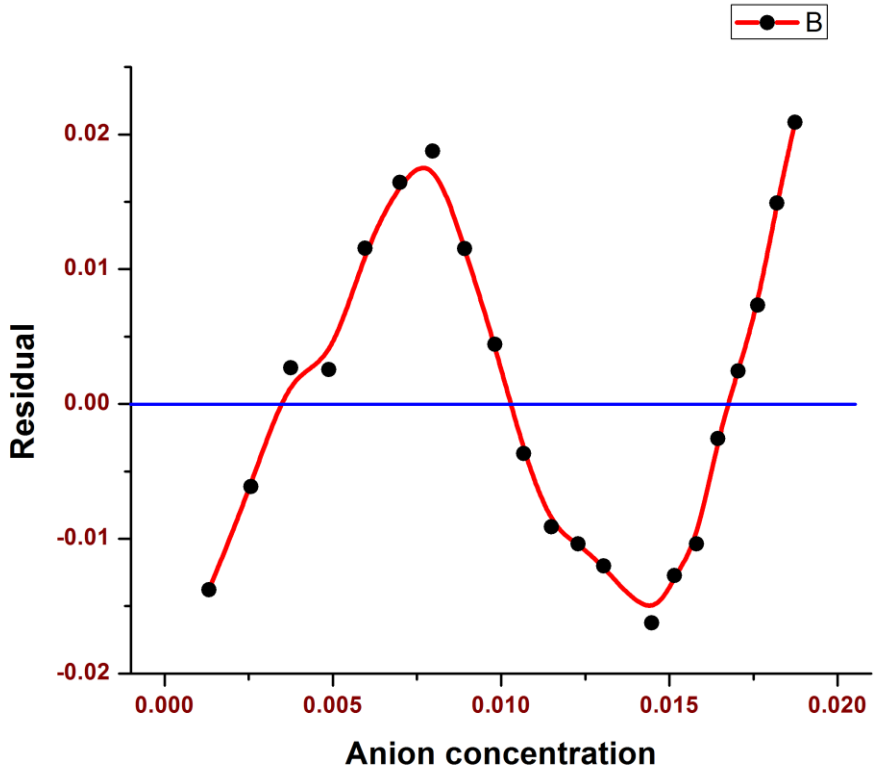

Fig. 55S: Residual plot of titration of **L3** *vs.* F^{-} in DMSO-d_6 at 298K.

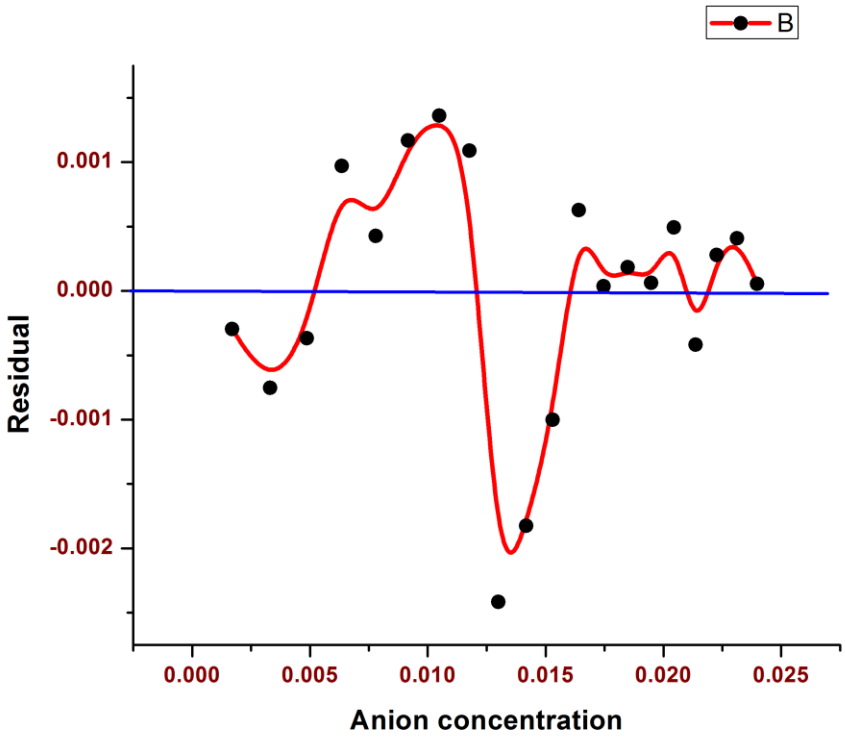

Fig. 56S: Residual plot of titration of **L4** vs. AcO^{-} in DMSO-d_6 at 298K.

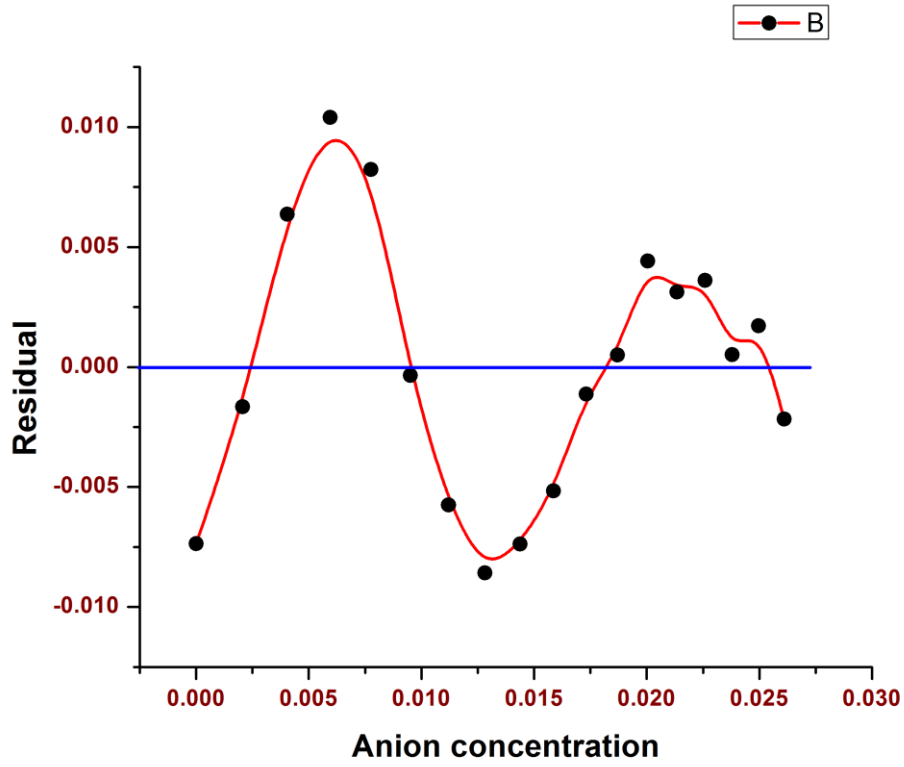

Fig. 57S: Residual plot of titration of **L4** *vs.* F^{-} in DMSO-d_6 at 298K.

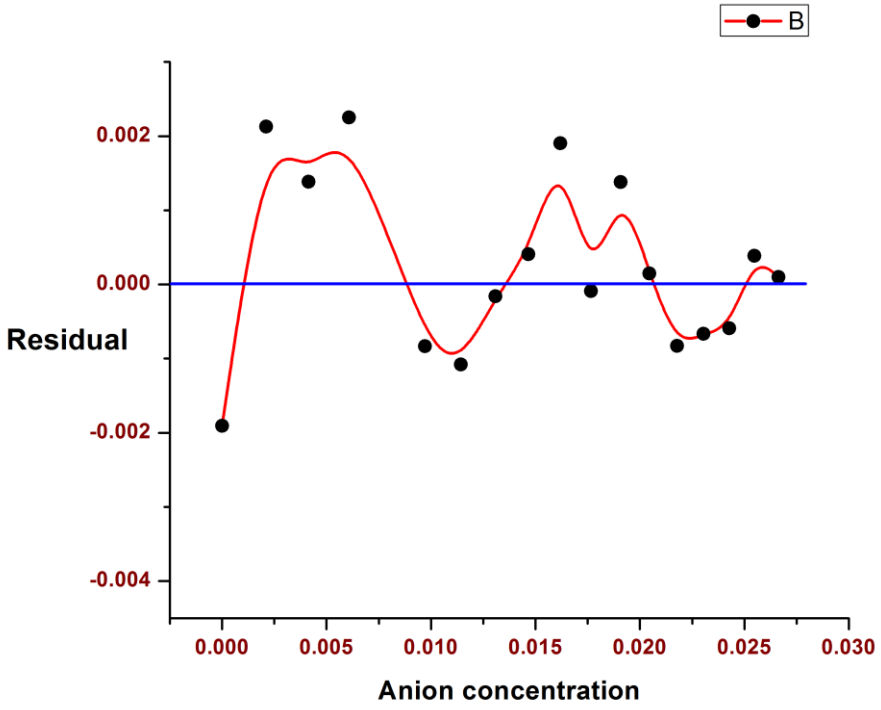

Fig. 58S: Residual plot of titration of **L5** vs. AcO^{-} in DMSO-d_6 at 298K.

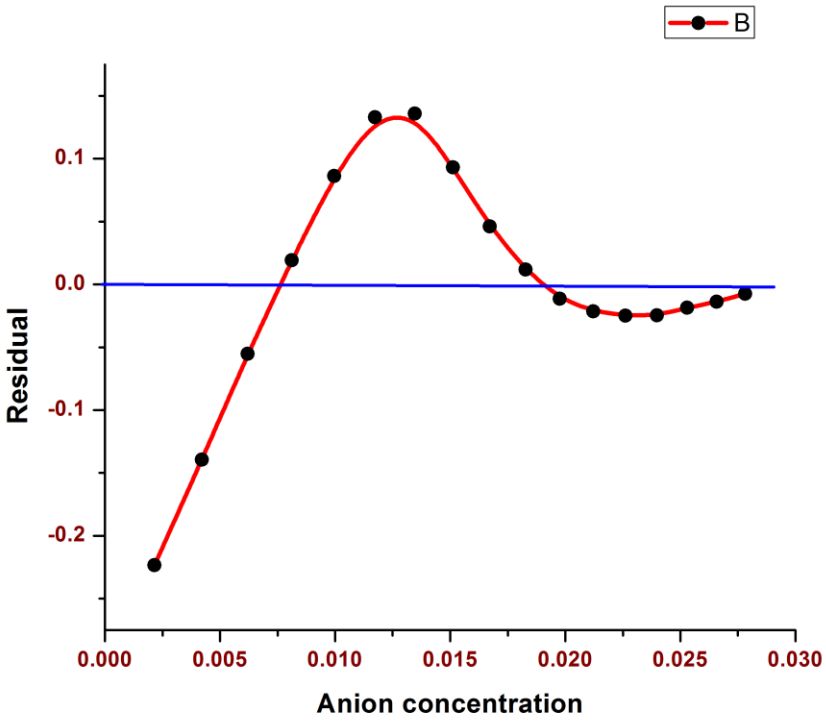

Fig. 59S: Residual plot of titration of **L5** *vs.* F^{-} in DMSO-d_6 at 298K.

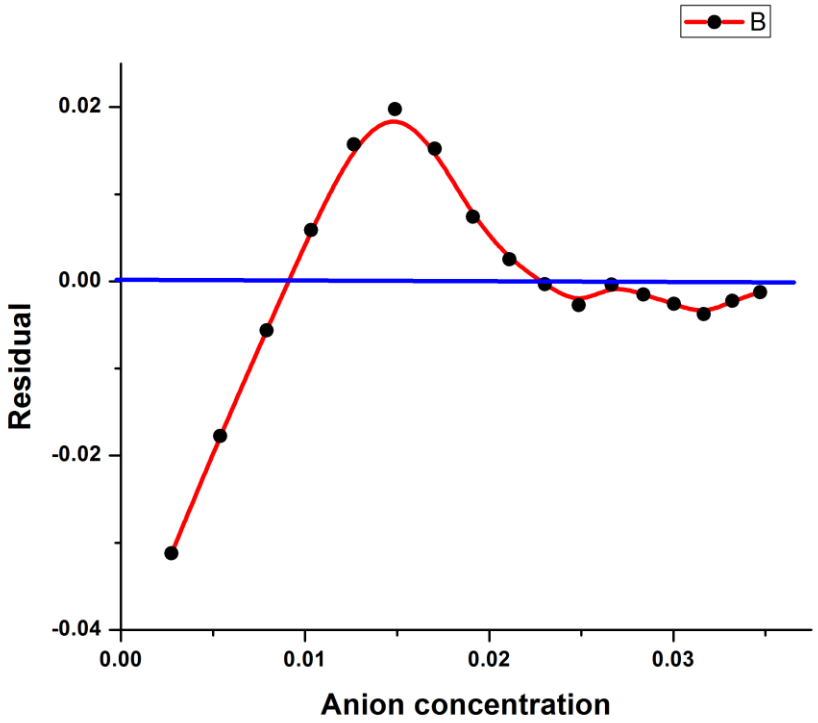

Fig. 60S: Residual plot of titration of **L6** vs. AcO^{-} in DMSO-d_6 at 298K.

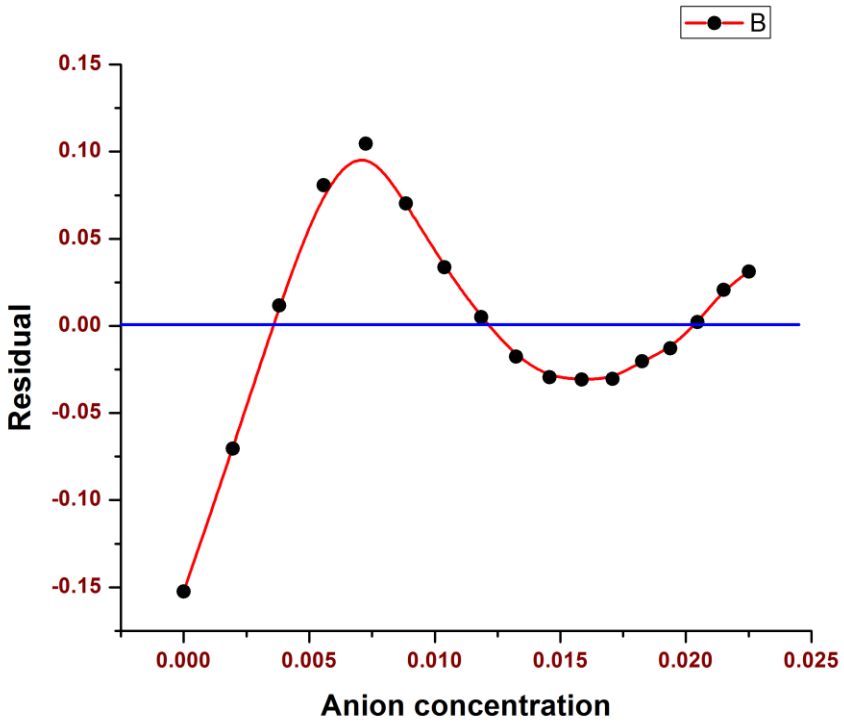

Fig. 61S: Residual plot of titration of **L6** *vs.* F^- in DMSO-d_6 at 298K.

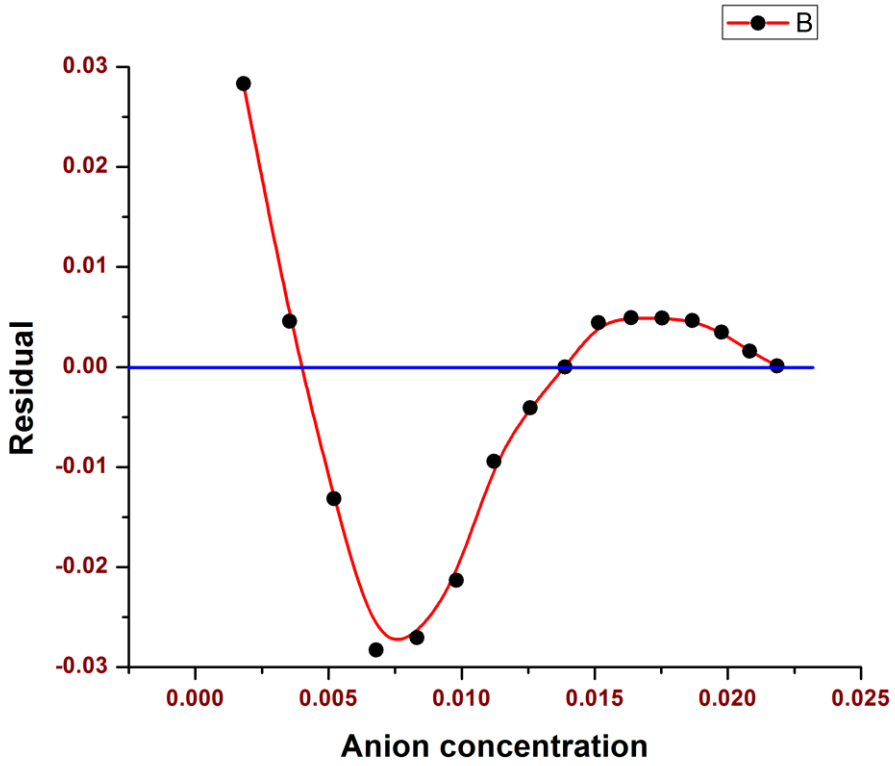

Fig. 62S: Residual plot of titration of **L7** vs. AcO^- in DMSO-d_6 at 298K.

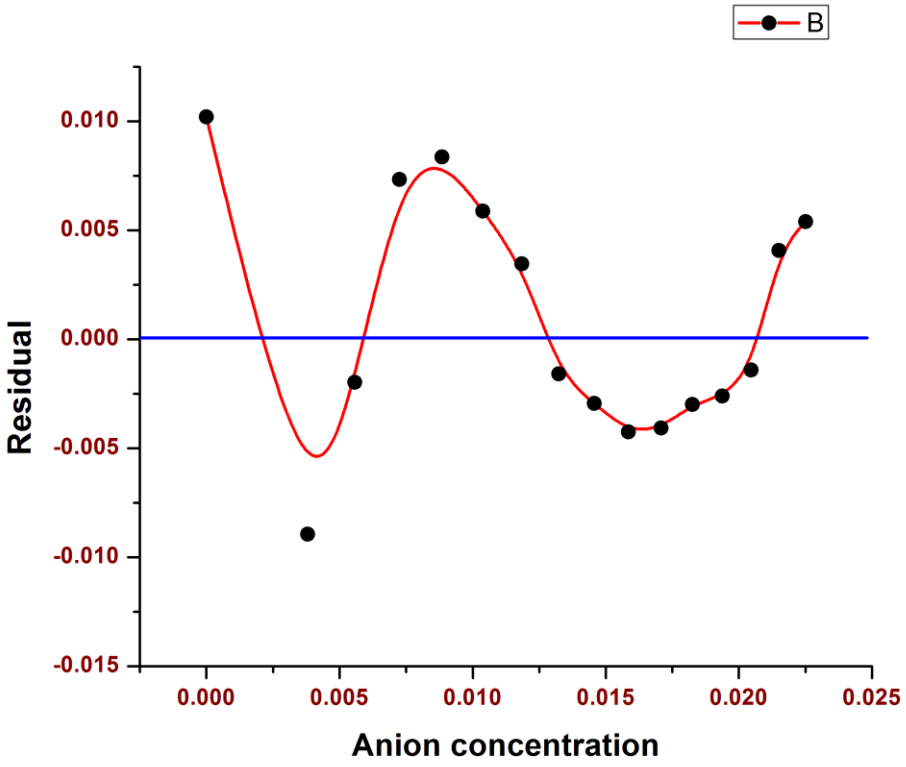

Fig. 63S: Residual plot of titration of **L6** *vs.* F^{-} in DMSO-d_6 at 298K.

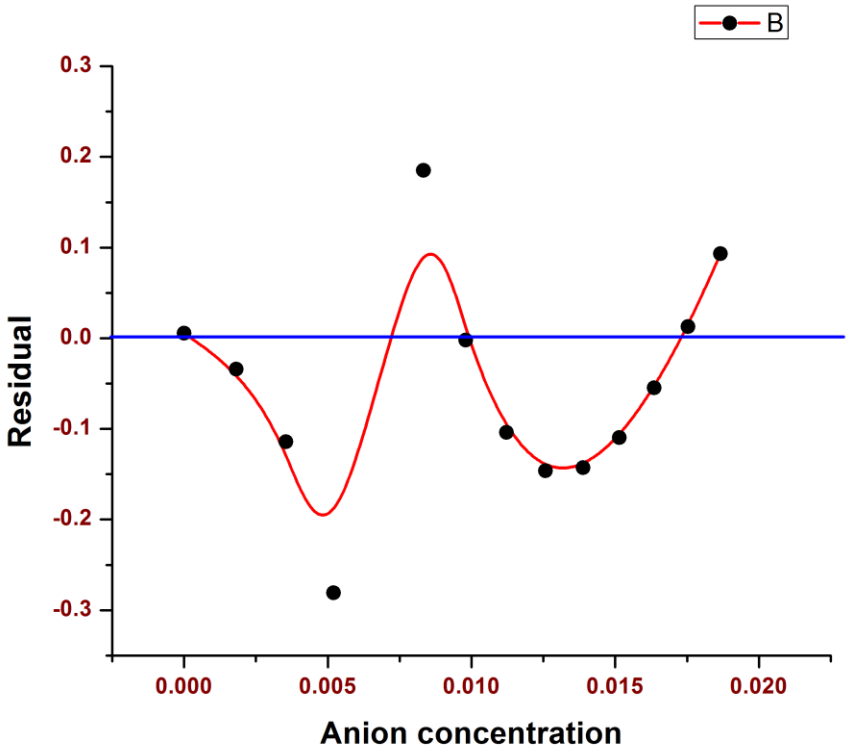

Fig. 64S: Job's plot of **L3** *vs.* AcO^{-} in DMSO-d_6 at 298K.

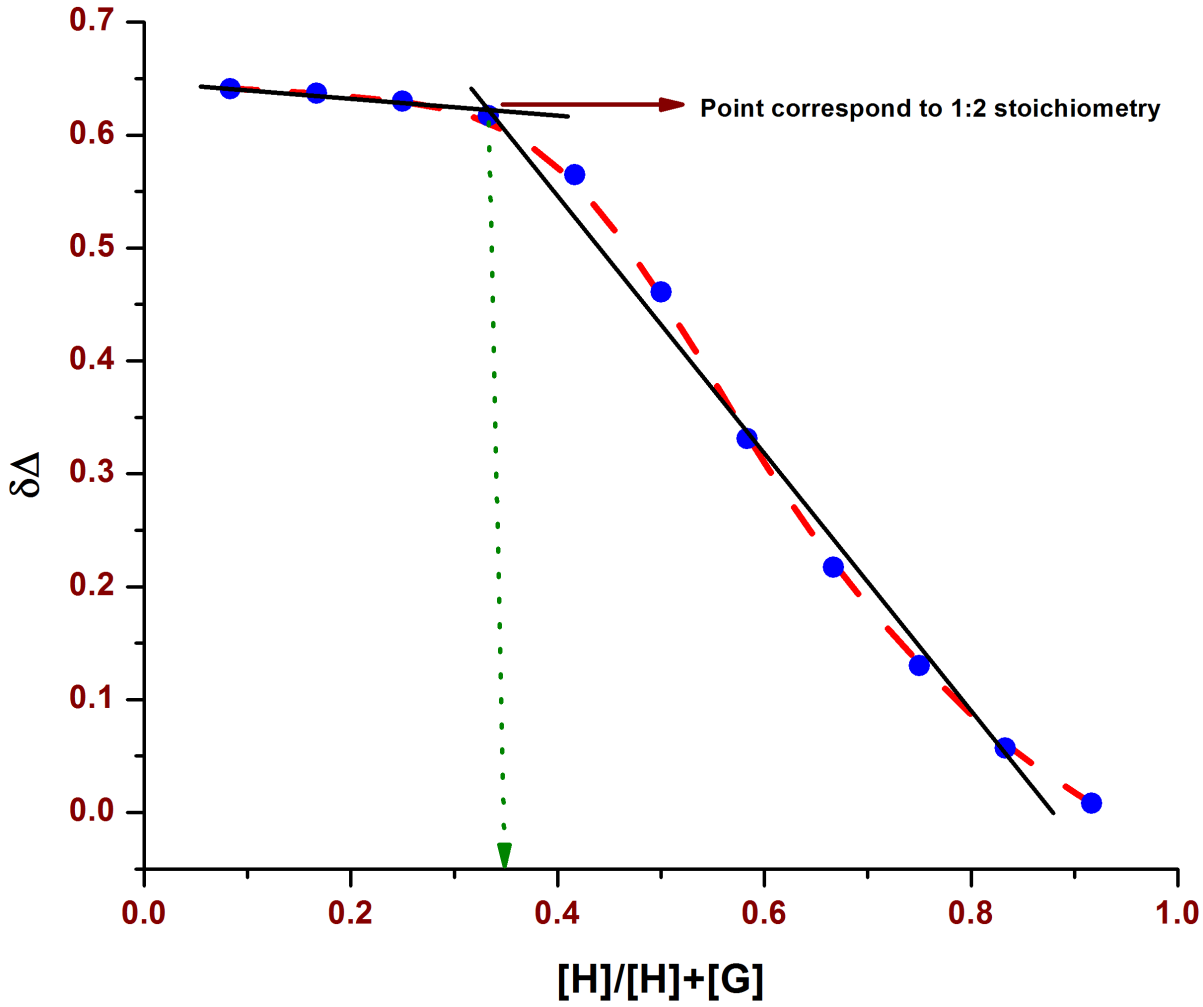

Volume of the Ligand (**L3**)	Volume of TBAAcO	Stoichiometry (H/G)
600 µL	0 µL	**0**
550 µL	50 µL	**11:1**
500 µL	100 µL	**5:1**
450 µL	150 µL	**3:1**
400 µL	200 µL	**2:1**
350 µL	250 µL	**7:5**
300 µL	300 µL	**1:1**
250 µL	350 µL	**5:7**
200 µL	**400 µL**	**1:2**
150 µL	450 µL	**1:3**
100 µL	500 µL	**1:5**
50 µL	550 µL	**1:11**

Fig. 65S: Job's plot of **L3** *vs.* F^- in DMSO-d_6 at 298K.

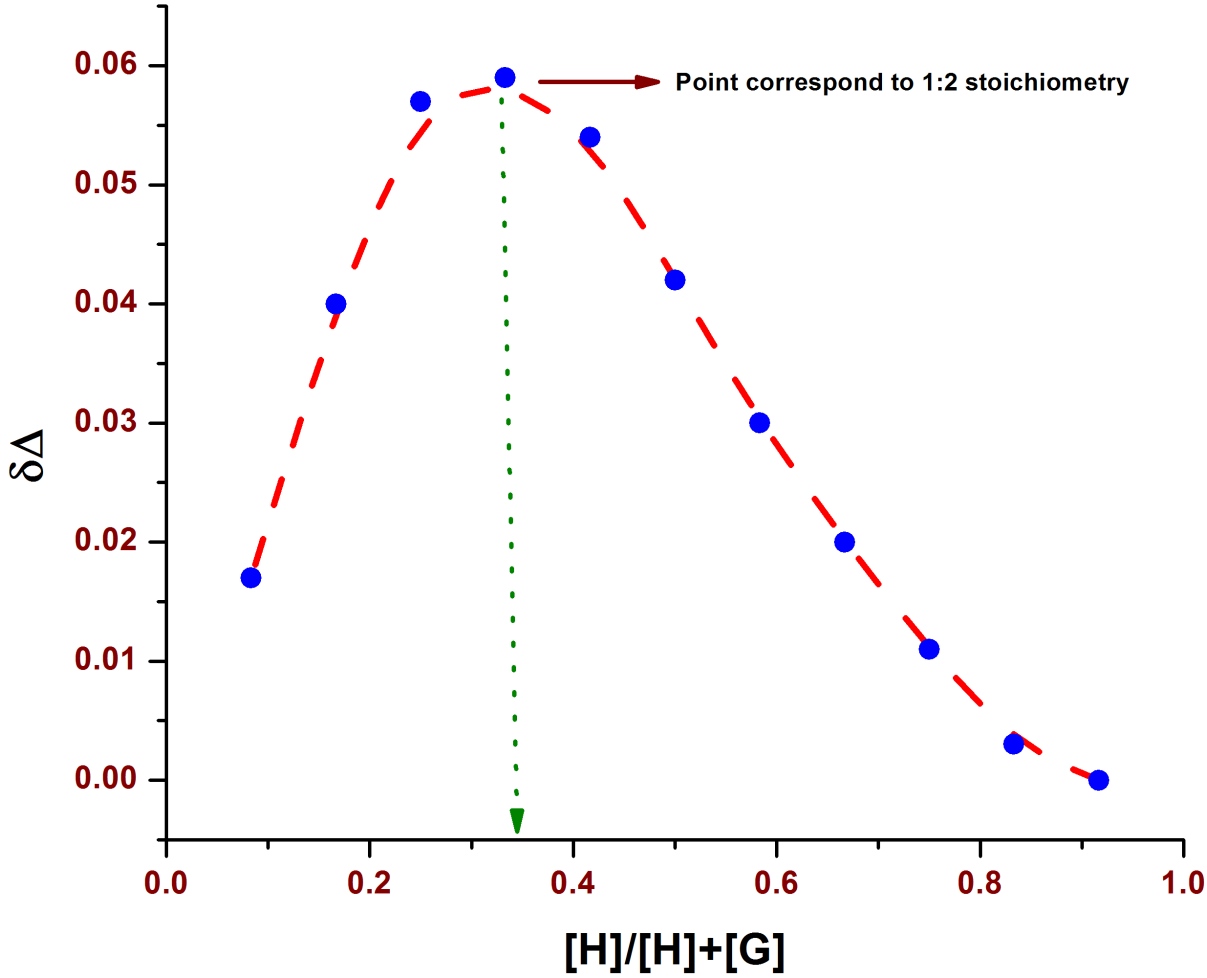

Volume of the Ligand (**L3**)	Volume of TBAF	Stoichiometry (H/G)
600 µL	0 µL	**0**
550 µL	50 µL	**11:1**
500 µL	100 µL	**5:1**
450 µL	150 µL	**3:1**
400 µL	200 µL	**2:1**
350 µL	250 µL	**7:5**
300 µL	300 µL	**1:1**
250 µL	350 µL	**5:7**
200 µL	**400 µL**	**1:2**
150 µL	450 µL	**1:3**
100 µL	500 µL	**1:5**
50 µL	550 µL	**1:11**

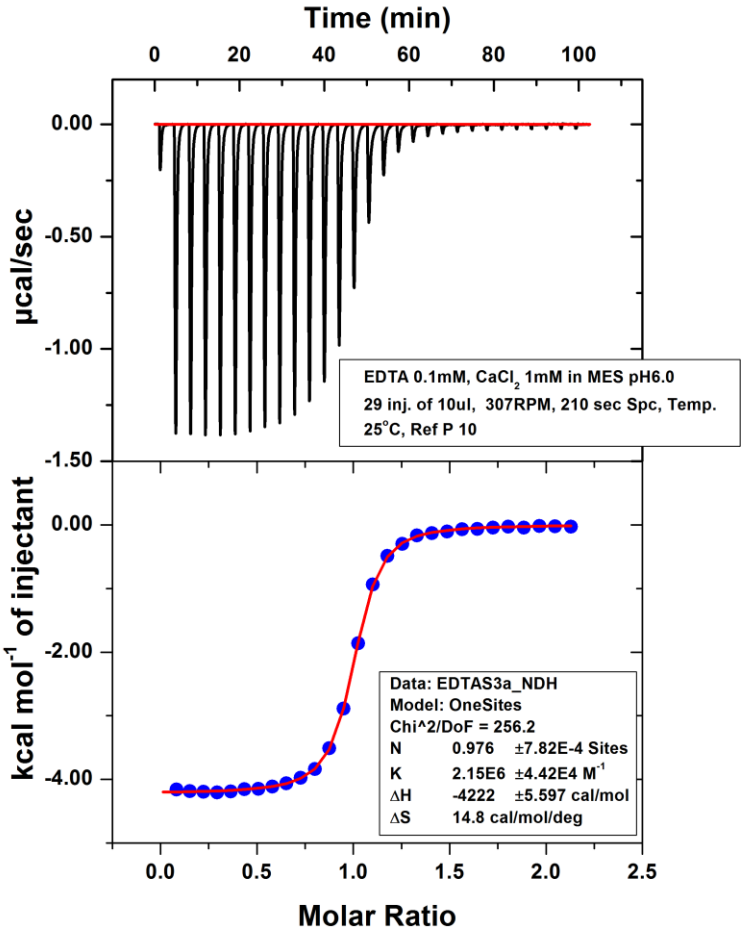

Fig. 66S: ITC accuracy check experiment with EDTA and $CaCl_2$ in MES buffer at pH = 6.0.